Zircon (U-Th)/He Thermochronometry

Peter W. Reiners

Department of Geology and Geophysics
Yale University
New Haven, Connecticut, 06520, U.S.A.
peter.reiners@yale.edu

INTRODUCTION

A number of features of zircon ($ZrSiO_4$), including high U-Th concentrations, high abundance in a wide range of lithologies, refractory nature under metamorphic and some magmatic conditions, and resistance to physical and chemical weathering, make it highly suitable for geochronology and thermochronology and thus a versatile tool for examining a wide range of earth processes. Like apatite and many other minerals, radioisotopic dating of zircon was first performed using the (U-Th)/He system, but the thermochronologic significance of zircon He ages has emerged only in the last few years. In this chapter, I review the current status of zircon He dating in the earth sciences, primarily as applied to thermochronology, including the controls on He diffusivity, the role of radiation damage, analytical techniques for measuring zircon He ages, special considerations unique to zircon He dating, and a series of case studies. Several examples from the literature are briefly summarized to illustrate the diversity of geologic problems accessible by zircon He dating and highlight the future potential of the system and outstanding unresolved issues. Exemplary applications include determining the timing and rates of orogenic exhumation and constraining provenance, depositional ages, and source terrain histories using He-Pb double dating of detrital zircons.

Historical perspective

Previous geo- and thermochronometric studies of zircon have utilized a wide range of decay schemes, including Pb-α (e.g., Webber et al. 1956), U/Pb, Pb/Pb, Th/Pb (Larsen et al. 1952; Vinogradov et al. 1952; Tilton et al. 1955; Wetherill 1955; Silver and Deutsch 1963; Parrish and Noble 2003; Ireland and Williams 2003; Bowring and Schmitz 2003), U-series (Scharer 1984; Reid et al. 1997), fission-track (Naeser et al. 1981; Brandon and Vance 1992; Bernet and Garver 2005; Tagami 2005), Lu/Hf (in concert with other phases; e.g., Pettingill and Patchett 1981), Sm/Nd (Futa 1986; Wernicke and Getty 1997), and $^{244}Pu/^{136}Xe$ (Turner et al. 2004). As with many other minerals, however, zircon was first dated using the (U-Th)/He system (Strutt 1910a,b). Strutt's pioneering work came not long after Ernest Rutherford reported the first radioisotopic age of any type, using He dating. Along with iron ores, titanite, and other minerals, Strutt measured He ages in zircons from a wide range of localities, reporting dates as young as 100 ka for zircons from Mt. Vesuvius, to as old as 565 Ma for a zircon from Ontario, Canada. Unlike some of his contemporaries, Strutt recognized that both U and Th produced He. Like others at the time, however, he also recognized that He ages were, in general, "minimum values, because He leaks out from the mineral, to what extent it is impossible to say" (Strutt 1910c). Not comfortable with attributing geochronologic significance to these apparent ages, Strutt generally referred to ages determined from relative He and U-Th measurements as "helium ratios."

Other early studies measuring zircon He ages include Holmes and Paneth (1936), who measured Oligo-Miocene ages for xenocrystic zircons in South Africa kimberlites, Larsen

and Keevil (1942), reporting a zircon He age of 23 Ma for the Lakeview tonalite in southern California, and Keevil et al. (1944) with a zircon He age of 260 Ma for the Chelmsford granite in Massachusetts. A number of studies led by Patrick Hurley (Hurley 1952, 1954; Hurley and Fairbairn 1953; Hurley et al. 1956) reported zircon He ages from a wide variety of locations and tectonic settings. Some of the more notable of these include He ages of 435–495 Ma for detrital zircons with relatively low U concentrations from Sri Lanka, and a much younger age of 130 Ma for a single specimen from this suite with much higher U content (Hurley et al. 1956). Hurley (1954) also reported numerous zircon He ages of 63–82 Ma from batholithic rocks in the Sierra Nevada, Idaho batholith, and southern California, and numerous zircon He ages of 650–880 Ma from Ontario. In 1957, Damon and Kulp reported zircon He ages from Ontario and Sri Lankan zircons, though their results on the latter suite were generally older than both previous and more recent studies.

By the 1950s it was generally clear that progress in (U-Th)/He chronometry would require a better understanding of the phenomena leading to natural He loss and ages younger than known or presumed formation ages. For some reason, however, most studies emphasized the role of radiation damage, rather than thermally activated diffusion, in observed variations of natural He loss. Several studies emphasized correlations between indices of radiation damage and apparent He retention among zircons from a cogenetic or geographically localized suite. Holland (1954) showed good correlations between natural radiation dosage and density and a unit cell parameter in Sri Lankan zircons. Holland noted that zircon density changed most rapidly after dosages of about 2×10^{18} α/g. He also noted, on the basis of work by Seitz (1949), that the number of atoms displaced by parent nuclide alpha-decay recoil for a dosage of this magnitude would be about 2×10^{21} displacements/g, about the same as the number of atoms per gram in zircon, thus demonstrating a "satisfactory agreement between the predicted and observed radiation dosage required for disordering the zircon structure completely."

Hurley and coworkers also examined relationships between radiation dosage, He age, refractive index, hardness, specific gravity, birefringence, and other crystallographic indices in zircon, with the hope of using an easily measured indicator of damage as a proxy for age (Hurley 1952; 1954; Hurley and Fairbairn 1953; Hurley et al. 1956). Such uses have not yet been developed, however, partly because it became clear, as was the case later with He retention, that the thermal history of zircons strongly affected the retention of radiation damage. In this work Hurley (1954) foreshadowed the development of (U-Th)/He thermochronometry in general by noting that in at least one region, He ages from a wide variety of minerals seemed to yield very similar ages despite widely varying radiation dosages and known He retentivities. He speculated that in such cases the minerals may "have accumulated helium only since some period of metamorphism."

Although the issue of radiation damage clouded recognition of the thermochronometric potential of (U-Th)/He dating in the early part of the 20th century, there were some early studies that attempted to quantify He diffusion rates in various minerals. Gerling (1939) measured the "heat of diffusion" (activation energy) of He diffusion in several different minerals, including monazite and uraninite, apparently finding increasing values for later stages of the experiments. For some reason, however, despite widespread use of closure concepts and thermochronometry based on other radioisotopic systems, clear recognition of the thermochronometric potential of (U-Th)/He dating did not develop until Zeitler et al.'s (1987) paper on apatite He dating. Subsequent work by Farley and coworkers developed the interpretational and methodological bases of apatite He dating (e.g., Wolf et al. 1996, 1998; Farley et al. 1996; Farley 2000). Subsequent work on other phases has developed experimental bases and methods for (U-Th)/He thermochronometry of titanite (Reiners and Farley 1999) and zircon (Reiners et al. 2002, 2004; Tagami et al. 2003), and shown the utility of these

methods in interpreting thermal histories of rocks from a variety of settings (e.g., Reiners et al. 2000, 2003; Stockli et al. 2000; Pik et al. 2003; Stockli and Farley 2004).

Apatite (U-Th)/He (apatite He) dating has received the bulk of attention in the thermochronologic community and in geologic applications, largely because of its uniquely low closure temperature (~60–70 °C for typical crystal sizes and orogenic cooling rates). At the time of writing of this volume, there are three existing reviews focusing on or including significant focus on apatite (U-Th)/He thermochronology (Farley 2002; Farley and Stockli 2002; Ehlers and Farley 2003). Although there have been some important development in apatite He dating since their publication, including insights from ^{4}He/^{3}He thermochronology (Shuster and Farley 2004, 2005; Shuster et al. 2004), here we focus on zircon He thermochronometry, although we show several examples of thermochronometric results combining apatite He, zircon He, and apatite and zircon fission-track (AFT and ZFT, respectively) data.

HELIUM DIFFUSION IN ZIRCON

Step-heating experiments

As in the case of apatite and titanite, understanding the thermal sensitivity of the zircon (U-Th)/He system relies primarily on results of step-heating experiments to determine He diffusion in zircon. Empirical studies of zircon He age patterns in natural settings with presumably well-understood thermal histories provide important complementary support, however. Reiners et al. (2002, 2004) presented He diffusion results from zircons with a range of ages and U concentrations. In most cases, cycled step-heating experiments on both whole unmodified crystals and interior chips of large gem-quality crystals yielded similar results, in which, following the initial ~5% degassing, activation energies (E_a) were 163–173 kJ/mol (39–41 kcal/mol) and log(D_0/a^2) were 3.7–4.7 s^{-1} (Fig. 1). These data also provide preliminary indications that, as in the case of apatite and titanite, physical grain size scales with diffusivity (i.e., the crystal size controls the lengthscale of the diffusion domain). Assuming that one half of the minimum dimension of a typical zircon crystal (i.e., the tetragonal prism half-width) corresponds to the diffusion domain lengthscale, then the D_0 derived from these experiments show a much smaller range than the D_0/a^2, with a range between 0.10–1.5 cm^2/s. Reiners et al. (2004) cited means and standard deviations of E_a and D_0 derived from the post-high-temperature heating parts of step-heating experiments as the best estimates for He diffusion in zircon. These were: E_a = 169 ± 3.8 kJ/mol (40.4 ± 0.9 kcal/mol), and D_0 = 0.46$^{+0.87}_{-0.30}$ cm^2/s. For typical igneous zircons with half-widths of ~40–100 μm, these diffusion parameters would yield closure temperatures (Dodson 1973) of 175–193 °C, for a cooling rates of 10 °C/m.y. (Fig. 2).

Reiners et al. (2004) showed that zircons with young He ages (~120 Ma) and low U concentrations (~100 ppm) display essentially identical diffusion characteristics as zircons with old He ages (~440 Ma) and very high U concentrations (~900 ppm). This is important because it suggests that at least in these cases the effects of radiation damage on He diffusivity do not become important until radiation dosages higher than about 2–4 × 10^{18} α/g, a level at which macroscopic and crystallographic characteristics of zircon also show large changes (e.g., Nasdala et al. 2001, 2004).

It is important to note that most available He diffusion experiments for zircon display anomalously high diffusivity in the earliest stages of step-heating. This behavior has also been observed in other minerals and is not well understood, and could have a range of origins, including effects from geometric vagaries of natural grain morphology, localized high-diffusivity from small high radiation-damage zones, crystallographically anisotropic diffusion, or inhomogeneously distributed He. Reiners et al. (2004) compared these non-Arrhenius features of the diffusion experiments with forward models of degassing from
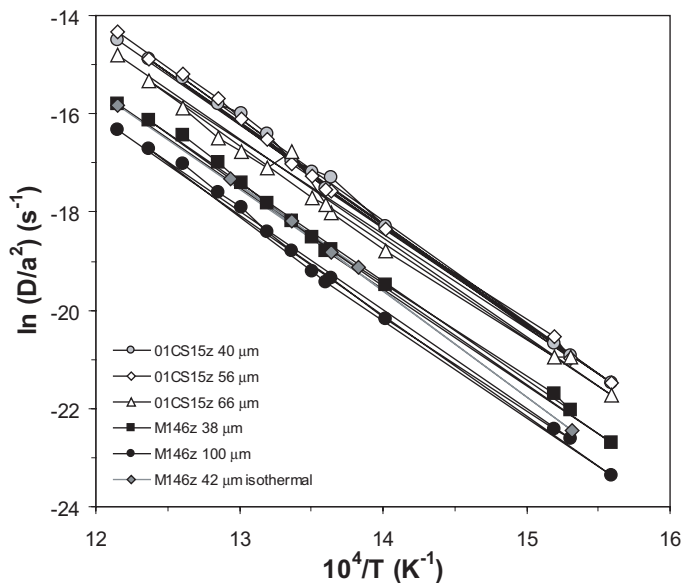
Figure 1. Arrhenius plot of post-high-temperature steps of cycled step-heating He diffusion experiments on different size fractions of two different zircon specimens, after Reiners et al. (2004). Early, low-temperature steps of each experiment displayed anomalously high diffusivity (not shown here), but these effects were absent after the initial steps at higher temperature (425–520 °C). Zircons from sample 01CS15z have a U/Pb age of ~122 Ma and zircon He cooling age of ~100 Ma, and U and Th concentrations of about 175 and 38 ppm, respectively. The sample from which these zircons came is the one at about 100 m from the dike in Figure 6. Specimens from M146z are fragments of a large gem-quality zircon with a U/Pb age of ~570 Ma and zircon He age of ~440 Ma, and U and Th concentrations of 923 and 411 ppm, respectively (Nasdala et al. 2004). Sizes quoted in inset are half-widths of minimum dimensions of individual crystals or crystal fragments. With one exception, data from smaller aliquots are shifted to systematically higher D/a^2, consistent with equivalency of diffusion domain size and grain size in zircon. These experiments indicate E_a = 163–173 kJ/mol (39–41 kcal/mol), and D_0 = 0.09–1.5 cm²/s, with an average E_a of 169 ± 3.8 kJ/mol (40.4 ± 0.9 kcal/mol) and average D_0 of 0.46 $^{+0.87}_{-0.30}$ cm²/s. For an effective grain radius of 60 μm and cooling rate of 10 °C/m.y., these yield closure temperatures, T_c, of 171–196 °C, with an average of 183 °C.

multiple domains of different sizes. These features could be matched well by positing small fractions of gas (2–4%) in domains with length-scales that are a factor of about 25–200 times smaller than the bulk grains themselves (Fig. 3). Zircons with a wide range of ages and radiation dosages exhibited approximately the same degree of non-Arrhenius behavior in initial diffusion steps. Although such modeling does not prove such a mechanism for these non-Arrhenius effects, it suggests that only a small proportion of gas resides in domains that exhibit anomalously high diffusivity, and therefore this phenomenon may not significantly affect the bulk closure temperature or He diffusion properties of most natural zircons.

Although Reiners et al. (2004) suggested that the anomalously high and non-Arrhenius diffusion seen in early stages of step heating experiments can be explained in ways that may not be important for most thermochronometric applications, this has yet to be proven. These and other features of He diffusion in zircon (and in other minerals) such as erratic behavior in some samples, are not easily explained and their origins may yet prove to be important in understanding anomalous ages and model thermal histories. One potential concern for step-heating diffusion studies of the type shown here, and which is common to most other He diffusion studies, is the possibility for crystallographic modifications during experiments
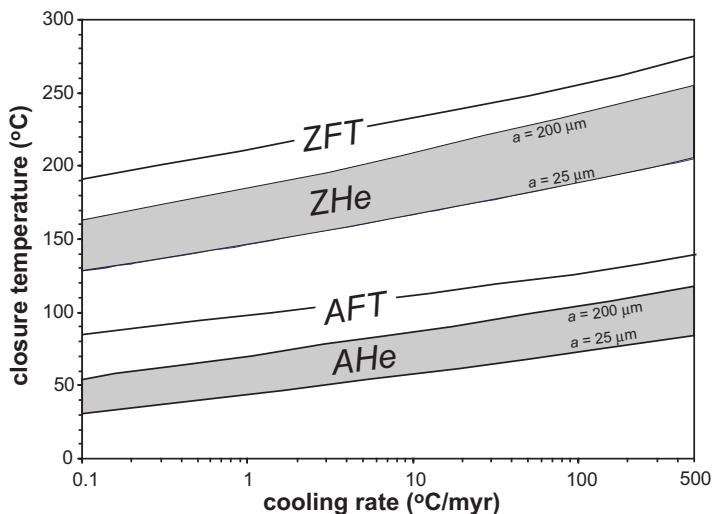
Figure 2. Closure temperatures calculated for apatite He and zircon He (Dodson 1973), using parameters from Farley (2000) and Reiners et al. (2004), respectively, and for AFT and ZFT [following approach of Bernet (2002), after Dodson (1979)] using parameters from Laslett et al. (1987) [$\beta = 9.83 \times 10^{11}$ s^{-1}, $E_a = $ 187 kJ/mol (44.6 kcal/mol)] and compiled data of Brandon and Vance (1992) [$\beta = 1.0 \times 10^8$ s^{-1}, $E_a = 208$ kJ/mol (49.8 kcal/mol)], respectively. Closure temperatures are calculated for large but not unreasonable potential variations in grain size for apatite He and zircon He, and cooling rates (a = diffusion domain size, corresponding roughly to the radius of a sphere with approximately the same surface-area-to-volume ratio as the crystal). AFT and ZFT closure temperatures are always higher than those for the (U-Th)/He system on the same minerals.

themselves. If heating at experimental temperatures and durations changes crystallographic features that affect diffusivity (e.g., by causing annealing), it is conceivable that such step-heating experiments may underestimate He diffusivity in natural zircons. Other important unresolved questions include the role of localized radiation damage zones in crystals whose bulk compositions would not suggest significant damage, the possibility of anisotropic diffusion, the interaction of microstructures, inclusions, or fission-tracks with migrating He, the possible role of pressure in He diffusion, and He solubility in zircon.

Radiation damage

As indicated by early studies relating radiation dosage and apparent (U-Th)/He ages, there is good evidence that He diffusion in zircon is strongly affected by relatively high degrees of radiation damage. This is most easily seen in suites of old zircons from a single sample (or from samples from a restricted region that experienced similar thermal histories) with a wide range of U concentrations. Detrital zircons from Sri Lanka, which presumably experienced similar thermal histories, show reproducible (U-Th)/He ages of 440 ± 9 Ma (2σ), and He diffusion characteristics similar to much younger and lower U zircons (Reiners et al. 2004), as long as U concentrations are less than ~1000 ppm. At higher U concentrations, zircon He ages decrease rapidly (Fig. 4). Zircons with high U concentrations also liberate He at high rates in vacuum, at low temperature (e.g., we have observed ~0.2 nmol ⁴He/g/min at room temperature, for a metamict zircon with ~5000 ppm U). The apparent cutoff at which low-temperature He diffusion rates dramatically increase corresponds to a radiation dosage, calculated from either (U-Th)/He age or U/Pb age, of about 2×10^{18} α/g, similar to the dosages at which Holland (1954) and Hurley et al. (1956) observed large changes in He diffusivity.
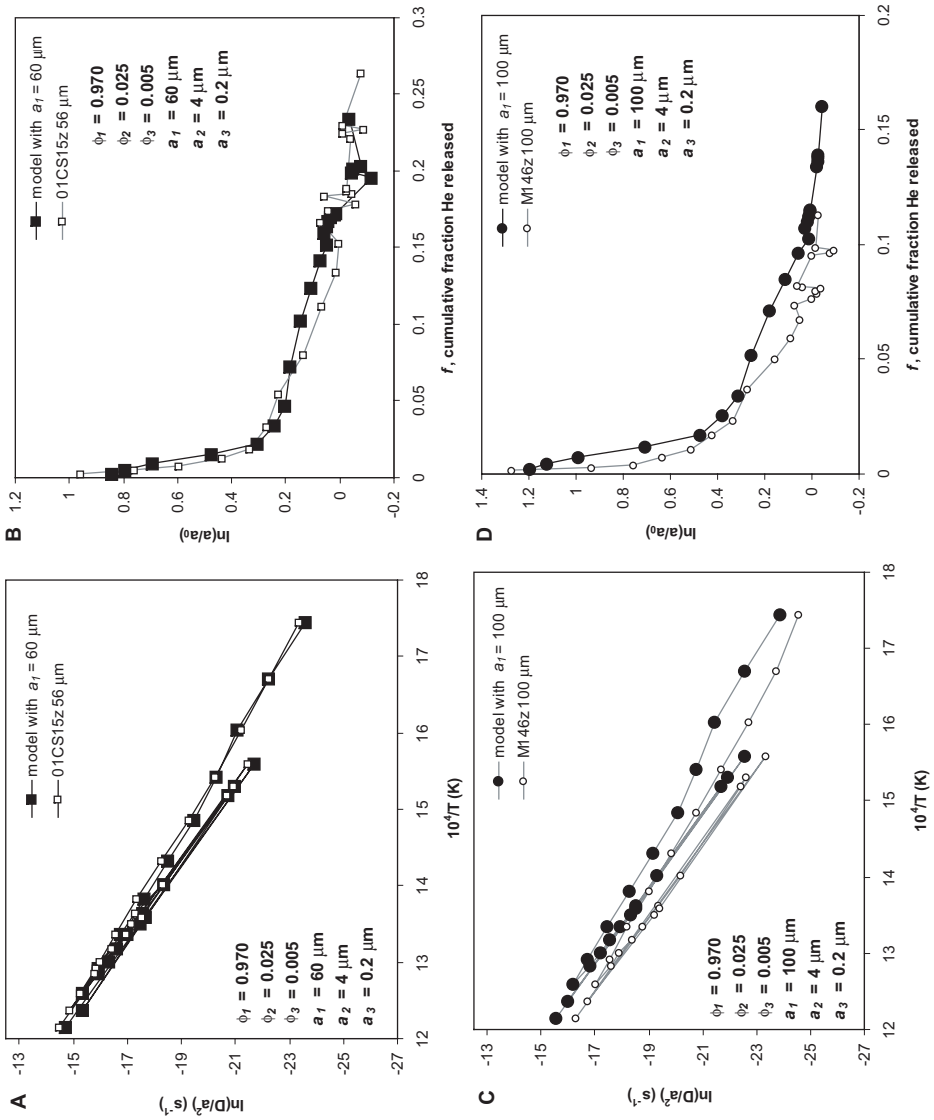
Figure 3. Arrhenius and $\ln(a/a_0)$ plots (see Reiners et al. 2004) from synthetic diffusion data predicted from three-domain diffusion models that reproduce observed data for natural zircons. Trends from two real experiments are shown for comparison. Assuming that only 2.5% and 0.5% of gas reside in domains that are factors of 25 and 200 smaller than the bulk grain, respectively, and using average E_a and D_0 derived from post-high-T portions of the diffusion experiments, closely reproduces the observed features of the Arrhenius trends.
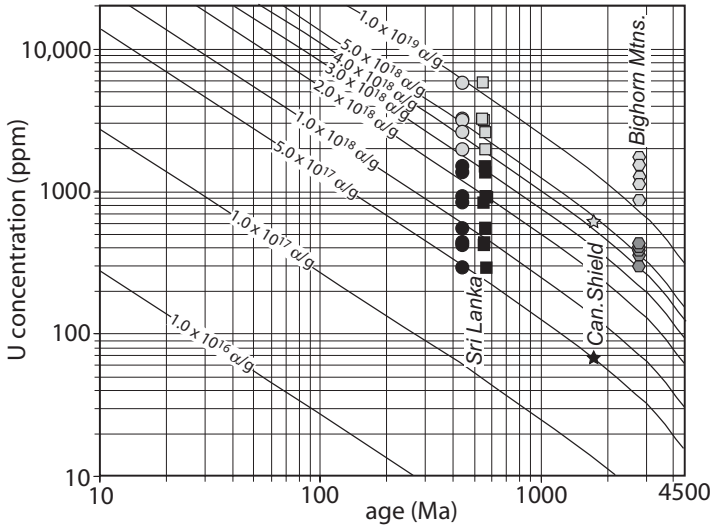
Figure 4. Contours of alpha dosage as a function of age and U concentration, assuming Th/U = 0.5, a typical value for zircon. Also shown are zircons from the detrital Sri Lankan suite studied by Nasdala et al. (2004) (circles), two zircons from the Canadian shield (stars; samples courtesy of Rebecca Flowers, MIT), and a suite of zircons from the Shell Canyon region of the Bighorn Mountains (octagons) (samples BH-12 and BH-17 of Reiners and Farley, 2001). Sri Lankan zircons are shown for both He age (442 Ma) and U/Pb age (555-560 Ma). Canadian shield and Bighorns zircons are shown for ^{40}Ar/^{39}Ar biotite cooling ages of 1.76 Ga and 2.8 Ga, respectively. Black symbols denote samples yielding zircon He ages that are reproducible and consistent with other thermochronologic constraints, implying insufficient accumulated radiation damage to affect the He age. Light grey symbols represent samples with anomalously young and unreproducible He ages, attributed to the effects of high radiation damage. Darker grey symbols for the low-U Bighorn samples denote samples with ages between 330–570 Ma; lighter grey symbols denote samples with ages between 7–178 Ma. None of these samples have reproducible zircon He ages at any U concentration, suggesting that they have all accumulated radiation damage sufficient to cause low-temperature He loss and anomalously young zircon He ages. In most suites of zircons, the transition from reproducible old ages to unreproducible young ages appears to occur at approximately $2–4 \times 10^{18}$ α/g.

Nasdala et al. (2004) and others have shown that the alpha-parent-recoil radiation damage responsible for metamictization is annealed at elevated temperatures. Although the kinetics of radiation damage are not well understood, it is clear that many zircons do not retain radiation damage that is simply proportional to their crystallization ages. In the case of the Sri Lankan suite, the retained radiation damage is only about one-half of that which would be accumulated since the U/Pb ages. This suggests that the critical radiation dosage for rapid low-temperature He loss in zircon should be calculated only for the duration of time a zircon has spent below some temperature at which damage is accumulated; in other words, from a cooling age rather than U/Pb age, though it is not yet clear exactly what temperature should be used for the cooling age.

Other suites of zircons with old U/Pb ages and relatively long low-temperature histories show similar results consistent with dramatically reduced He retentivity at higher radiation dosages. In some cases, it is not possible to estimate the extent of retained radiation dosage as a function of U-Th concentration, because no zircons at any U concentration provide reliable and reproducible He ages, and few if any other constraints are available on the low-temperature thermal histories. However in some cases, suites of zircons with wide ranges of U concentrations can be found in rocks with cooling age and thermal history constraints from other systems.

Such cases can be used to place at least some constraints on the effective radiation dosage at which low temperature He loss increases rapidly. Figure 4 shows U concentrations and cooling ages of several zircon suites in which single-crystal age measurements appear to cross a threshold of radiation damage leading to anomalously young and irreproducible He ages. These data also suggest that this low-temperature radiation accumulation limit lies somewhere between about $2–4 \times 10^{18}$ α/g. Assuming a critical retained dosage of 2×10^{18} α/g represents an effective upper dosage limit for meaningful (U-Th)/He ages, then typical zircons with U concentrations of about 100-1000 ppm would require full retention at low temperatures for at least 0.6 to 4.0 b.y.. Potentially more insidious effects of smaller degrees of radiation damage at intermediate temperatures are not yet known.

As noted by Nasdala et al. (2004), strong He diffusivity changes in zircon are observed at a critical accumulated radiation dosage corresponding to double-overlapping of alpha recoil damage zones (see also Nasdala et al. 2001). If the relationship between He diffusivity and alpha damage is also systematic at intermediate extents of damage (i.e., not just a critical threshold), it may be possible to use the specific relationship between alpha fluence and apparent (U-Th)/He age among zircons from the same rock to deduce thermal histories. Figure 5 shows the apparent zircon He ages as a function of alpha fluence for zircons from rocks with similar
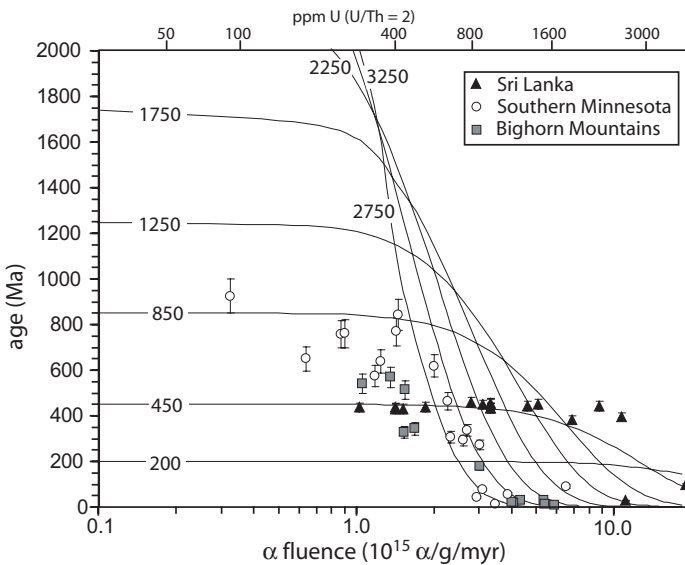

Figure 5. Measured zircon He age versus alpha fluence from measured U and Th concentrations for zircons from a range of settings. The upper *x*-axis is for reference, to denote U concentrations that would produce given alpha fluences for a U/Th of 2, typical of zircon; it does not denote actual U concentrations in these zircons. Zircons shown are: (1) the Sri Lankan suite of Nasdala et al. (2004), with crystallization and cooling ages of ~560 Ma and ~440 Ma, respectively; (2) granitoids of the Shell Canyon section, Bighorn mountains, Wyoming (Reiners and Farley 2001), with a crystallization age of ~2.8 Ga and an unknown age of cooling through the zircon He closure temperature (apatite He ages on the same samples require temperatures less than ~70 °C for at least the last ~600 m.y.); (3) granitoids and metamorphic rocks of the Minnesota river valley, with crystallization ages ranging from ~2.6–3.6 Ga and unknown cooling ages. Model trends are constructed to test the simple hypothesis that the ratio of observed to "actual" zircon He cooling age is equal to the fraction of remaining crystallinity in the zircon, where the latter is determined using the double-overlapping cascade model of Holland and Gottfried (1955). This simple model appears to work for the Sri Lankan zircons, but not for the older groups, suggesting a more complex relationship between He retention and fractional crystallinity from radiation damage.

thermal histories involving long-term residence at low temperatures (note that this analysis makes use of alpha fluence, or rate of production, not cumulative alpha dosage). Also shown in this figure are trends of zircon He ages that would be measured for zircons with the same original He cooling age, but varying radiation dosage, assuming that the ratio of observed zircon He age to actual cooling age is equal to the fraction of remaining crystallinity, where crystallinity is determined by the double-overlapping cascade model (Holland and Gottfried 1955). In the context of such a hypothetical model, zircons with young "actual" cooling ages would preserve geologically significant zircon He ages even at high alpha fluences, but with increasing "actual" cooling age, zircons with progressively lower alpha fluences would show decreasing apparent ages. The Sri Lankan zircon suite shows a trend that may be consistent with this model, with high fluence grains falling to lower ages than the inferred cooling age for these samples in approximate proportion to crystallinity. Other samples, from granitoids of southern Minnesota and the Bighorn Mountains of Wyoming, however, are not consistent with this simple model. At relatively high fluences, these zircons show age-fluence trends similar to the model trends for "actual" cooling ages of ~2.5–3.0 Ga, but at lower fluences, the ages are lower than expected for such trends. This may mean that He diffusivity does not scale linearly with crystallinity and/or alpha damage in zircon. More work is clearly needed to understand the relationships between radiation damage and He diffusivity, and to extract any potentially useful information in age-fluence relationships. It is worth noting again, however, that at least in the cases we have examined such as the Sri Lankan suite, radiation damage effects only become important at fairly high accumulated radiation dosages, requiring old ages, long-term residence at low temperatures, and relatively high U-Th concentrations.

ANALYTICAL AND AGE DETERMINATION TECHNIQUES

Analytical methods

Most (U-Th)/He dating procedures involve measurement of parent and daughter nuclides on the same aliquots, because of the potential for varying U and Th concentrations among crystals. Single aliquot measurements are particularly important for zircon He dating, because U and Th concentrations among zircon crystals often show large variations. Currently, measurement of a reasonably precise He age using routine methods in the Yale (U-Th)/He chronometry lab typically requires ^{4}He contents at least as high as about 0.3 fmol. For a typical zircon of about 200 μm length and 100 μm width, with 350 ppm U and U/Th ~2, this requires only about 20 kyr of ingrowth. Thus, most zircon He applications require only single crystals, though it is conceivable that some applications, such as dating of very young or low-U-Th samples may be better suited to multi-crystal aliquots. Ideally, at least two single crystal replicates of zircons are dated (many more are dated if the sample comprises unreset detrital grains), to check reproducibility of single grain ages. The procedures described here are those employed for routine zircon He dating in the Yale (U-Th)/He chronometry lab, and may differ from protocols in other labs.

Crystal selection, documentation, and alpha-ejection corrections. Dated crystals are selected from heavy mineral separates prepared by standard procedures, on the basis of size, morphology, abundance of inclusions, and clarity. The following selection guidelines apply to non-detrital zircons, where there is no risk of biasing age populations by grain selection criteria. In general, suitable crystals have tetragonal prism widths of at least 75–90 μm. As a general rule of thumb, except in rare circumstances crystals with tetragonal prism widths less than 60 μm are not dated, because uncertainties in the very large alpha-ejection corrections (and inherent assumptions about parent zonation required in conventional analyses) can lead to potentially large errors. Interestingly, however, Hourigan et al. (2005) noted that U-Th zonation effects on age inaccuracy actually decrease at crystal sizes less than ~60 μm, because

at such small sizes, all parts of the crystal are affected by alpha ejection roughly equally. The potential disadvantage of extremely large crystals (e.g., ~300 μm widths), however, is that they may require multiple heating and gas extractions to reduce subsequent extractions to less than ~2% of the total, and such large grains occasionally also show dissolution problems. Thus optimally sized crystals for routine zircon He dating procedures have tetragonal prism widths of about 75–150 μm.

Alpha-ejection corrections (described below) require an assumption of a characteristic grain morphology, so in many cases grains with morphologies most similar to an idealized tetragonal prism with bipyramidal terminations are selected. Other suitable morphologies include regular prolate spheroids or tetragonal prisms with broken ends perpendicular to the *c*-axis. In general, however, highly irregular morphologies or grains with obviously fractured surfaces at low angles to the *c*-axis are avoided. In most samples, it is difficult to select zircons without any inclusions, but in order to minimize potential zonation effects, grains with few large or obvious inclusions are selected.

Selected crystals are photographed and their dimensions are measured in at least two mutually perpendicular perspectives parallel to the a_1 and a_2 crystallographic axes. These dimensions and an assigned morphology are used to calculate the alpha-ejection correction, to account for ^{4}He lost from the crystal by long-stopping distances of alpha-particles. In zircon, stopping distances average about 17.0 μm for the ^{238}U series, 19.6 for the ^{235}U series, and 19.3 for the ^{232}Th series (Farley et al. 1996; Hourigan et al. 2005). Farley (2002) provided equations for zircon alpha-ejection corrections based on assumed crystal morphologies of tetragonal prisms with pinacoidal terminations. This approach used Monte-Carlo modeling to parameterize second order polynomial factors as a function of crystal surface-area-to-volume ratio β, to solve for fractions of He retained within the crystal for the U- and Th-series individually. Measured Th/U of individual zircons are then used to weight the series' specific retention factors appropriately. This approach has been used in most zircon He dating studies, and provides accurate ages for standards of known age (Kirby et al. 2002; Reiners et al. 2002, 2003, 2004; Tagami et al. 2003).

As part of a larger study examining intracrystalline U-Th zonation in zircon He dating, Hourigan et al. (2005) examined the effects of more realistic crystal geometries on alpha-ejection correction. They found that bipyramidal terminations generally have the effect of changing alpha-ejection corrections from those calculated assuming pinacoidal terminations by about 1–3%. The magnitude of the discrepancy is proportional to the fraction of the total *c*-axis parallel length of the crystal comprising the pyramidal tips. Typical zircons have pyramidal terminations that are about 10–30% of the total length, although considerable variation exists in natural crystals. Using this more realistic morphology, Hourigan et al. (2005) determined new factors for the polynomial on β for determining fraction of He retained in the crystal. Table 1 shows the U- and Th-series factors determined in that study.

The surface-area-to-volume ratio β, is calculated from equations shown in Table 2. Some natural zircons, especially those in sedimentary environments, are well rounded and bear more resemblance to prolate spheroids than to tetragonal prisms with or without pyramidal terminations. In such cases, measurements of equatorial and polar radii are made (with a mean equatorial radius determined from the average of two mutually perpendicular measurements), and different equations are used for surface-area and volume calculations (Table 2).

Although concentration determinations of neither parent nor daughter are required for He age determinations, most studies report estimated U and Th concentrations of dated crystals. This can be useful in several ways, including assessing radiation damage effects, identifying anomalous crystals, or elucidating zonation from He-Pb double-dating results (Reiners et al. 2005). Because single crystal aliquots are typically too small to precisely weigh by standard

Table 1. Factors A_1 and A_2 for calculating fraction of He retained in crystals from the ^{238}U and ^{232}Th decay series in zircon, for different assumed crystal geometries.

| | Tetrahedral prism with pinacoidal terminations | | | | Tetrahedral prism with pyramidal terminations | |
| | (Farley 2002) | | (Hourigan et al. 2005) | | (Hourigan et al. 2005) | |
Parent Nuclide	A_1	A_2	A_1	A_2	A_1	A_2
^{238}U	−4.31	4.92	−4.35	5.47	−4.28	4.37
^{232}Th	−5.00	6.80	−4.94	6.88	−4.87	5.61

Table 2. Surface areas and volumes of zircons for assumed geometries of zircon crystals.

Geometry	Volume	Surface Area
Tetragonal* prism with pyramidal terminations	$V_z = 4\, r_1 r_2 \left[(l - h_1 - h_2) + \dfrac{1}{3}(h_1 + h_2) \right]$	$SA_z = 4(l - h_1 - h_2)(r_1 + r_2) + 2r_1 a + 2r_2 b$ $a = \sqrt{h_1^2 + r_2^2} + \sqrt{h_2^2 + r_2^2}$ $b = \sqrt{h_1^2 + r_1^2} + \sqrt{h_2^2 + r_1^2}$
Prolate Spheroid	$V_{ps} = \dfrac{2}{3}\pi r^2 l$	$SA_{ps} = 2\pi r^2 + \left[\dfrac{2\pi r \left(l/2\right)^2}{\sqrt{\left(l/2\right)^2 - r^2}} \right] \sin^{-1}\left[\dfrac{\sqrt{\left(l/2\right)^2 - r^2}}{\left(l/2\right)} \right]$

Note: l = c-axis-parallel length; h_1, h_2 = pyramidal termination lengths; r_1, r_2 = mutually-perpendicular prism half-widths or average equatorial radius. Prolate spheroid geometry was not modeled for independent polynomial factors, and is assumed to have the same A's as the tetragonal prism with pyramidal terminations.

*Although the Monte Carlo models are derived from tetragonal prism morphologies, differing prism half-widths are typically measured to calculate volumes and surface areas, because typical zircons are commonly significantly orthogonal.

techniques, mass estimates for concentrations are determined from volume estimates, assuming an average density, for which we use 4.6 g/cm^3 for zircon. Given that grain dimension measurements typically include length, widths, and, if pyramidal terminations are considered, their lengths, or else polar and equatorial radii, the morphological assumption used for volume calculation has a large effect on estimated mass. Using realistic morphologies as opposed to simplified tetragonal prisms with pinacoidal terminations results in estimated volumes and masses that are typically 10–50% lower (Reiners et al. 2005).

In summary, alpha-ejection corrections are made in the following way. Following Farley et al. (1996) and Farley (2002), the fraction of He retained in crystals due to alpha-ejection (F_{He}) for ^{238}U and ^{232}Th (^{235}U is similar to ^{232}Th) are calculated from a polynomial fit to surface-area-to-volume ratios and fraction of alphas retained in the crystal, where:

$$F_{He} = 1 + A_1\beta + A_2\beta^2 \tag{1}$$

where A_1 and A_2 are given for different morphologies in Table 1. The F_{He} for each nuclide is then weighted according to the measured Th/U of the sample, to derive the bulk F_{He}, using the equations:

$$\hat{F}_{\text{He}} = a_{238} \, {}^{238\text{U}}F_{\text{He}} + (1 - a_{238}) \, {}^{232\text{Th}}F_{\text{He}} \tag{2}$$

and

$$a_{238} = (1.04 + 0.245(\text{Th}/\text{U}))^{-1} \tag{3}$$

Extraction and measurement of He, U, and Th. Early analytical procedures extracted He from zircons by either *in vacuo* fluxing or heating of crystals in small (~5 mm) stainless steel or Ti capsules in a resistance furnace at ~1200–1300 °C (Reiners et al. 2002). Although the latter method was successful in most cases, disadvantages include potential loss of material for U-Th analyses upon retrieval from the capsules, as well as the relatively high He blanks and time-consuming temperature cycling of furnace heating, compared with laser heating. Routine He extraction techniques in the Yale lab now typically involve placement of a single crystal into a small (~1 mm) Nb foil envelope that is lightly crimped closed, and heating of the foil by direct lasing with a focused 10 μm beam of a 1064-nm Nd:YAG laser. The foil sits in a Cu or stainless steel planchet with a few dozen sample slots, directly underneath a KBr coverslip, which prevents vapor deposition on the underside of a sapphire viewport above the samples, in a high-vacuum sample chamber connected to the He purification/measurement line. Nb foils are heated to approximately 1100–1250 °C for 15 minute extraction intervals; all samples are then subject to at least two and occasionally more extractions and He measurements, to assess the extent of degassing of the crystal. Typically, re-extracts yield less than 0.5% of previous ^{4}He yields, but some zircons can display stubborn He extraction, with multiple extracts required to reduced successive yields to less than 2–3%. It is not known why some zircons display such reticent He extraction during laser heating (it is not obviously related to radiation dosage, thermal history, U-Th content, for example), or whether this reflects unusual He diffusion properties during natural cooling as well.

Gas extracted from zircons by heating is spiked with approximately 0.1–1.0 pmol ^{3}He, cryogenically (and/or via gettering) concentrated and purified, and expanded into a small volume with a gas-source quadrupole mass spectrometer. The ^{4}He/^{3}He is measured for about ten seconds following gas release and nominal equilibration time. The measured ratio is corrected for background and interferences on mass 3 (HD$^+$ and H$_3^+$), and compared with the ^{4}He/^{3}He measured on pipetted aliquots of a manometrically calibrated ^{4}He standard processed by the same methods. ^{4}He in the unknown zircon is assumed to be the product of the ^{4}He content of the standard with the ratio of the ^{4}He/^{3}He measurements on the unknown and the standard. Linearity of this calibration approach has been confirmed in the Yale He lines over about four orders of magnitude of ^{4}He signal. Each batch of zircons is processed with several "hot blanks" and "line blanks" to check the measured ^{4}He/^{3}He of laser extraction procedures on empty Nb foil envelopes, and ^{4}He/^{3}He of ^{3}He-only shots. Nominal ^{4}He blanks from these procedures range between 0.05–0.1 fmol, although reproducibility of blanks, and therefore uncertainty on unknown He contents make precise determination of ^{4}He contents lower than roughly 0.3 fmol difficult.

Parent nuclide contents of degassed zircons are measured by isotope dilution and solution ICP-MS. This requires spiking with isotopically distinctive U-Th spike, sample-spike equilibration, and dissolution to a final solution suitable for ICP-MS. Zircon requires different dissolution techniques than those developed for apatite or titanite (House et al. 2000; Reiners and Farley 1999), because most zircons do not dissolve in nitric acid alone and require HF-HNO$_3$ mixtures at higher than ambient temperatures and pressures. Dissolution of zircon directly from Pt foil, as in the case of apatite, is not possible because of Pt dissolution, forming PtAr$^+$ complexes in the ICP-MS with isobaric interferences on U isotopes. In principle,

$^{195}Pt^{40}Ar$ and $^{198}Pt^{40}Ar$ could be resolved from ^{235}U and ^{238}U using high resolution, but the disadvantages of lower sensitivity, mass calibration, and triangular peak shape make avoidance of dissolved Pt in the solution a simpler option. House et al. (2000) used Pd foil for wrapping and laser-heating of titanite, and dissolved titanite directly from the foil in a spiked HCl-HF solution. In our experience however, the lower melting temperature of Pd made it more prone to melting during lasing, compromising quantitative recovery of the U-Th in the zircon. Rather than unwrapping Pt foils and retrieving naked zircons, which also potentially compromises quantitative parent recovery, an alternative procedure is to dissolve the entire Nb foil and contents in Parr pressure digestion vessels (Parr bombs). An alternative procedure, outlined by Tagami et al. (2003), involves flux melting of zircons in Pt foils in the presence of U-Th spike, and subsequent dissolution of the resulting glass for ICP-MS measurement. This procedure avoids time-intensive acid dissolution steps, but, at least as reported in Tagami et al. (2003), yields U-Th blanks about 4–25 times higher than those we observe for acid dissolution.

The first step of our U-Th measurement procedure is spiking of zircon-bearing Nb-foils with 0.4–0.8 ng of ^{233}U and 0.6–1.2 ng of ^{229}Th. In contrast to some apatites, the low Sm content of zircon generally does not lead to significant age contributions from this element. The foil and spike are initially bombed in Teflon vials at 225 °C for 72 hours. Samples are then heated to dryness and then rebombed and dissolved in HCl at 200 °C for 24 hours to redissolve refractory fluoride salts. After a final drydown the sample is redissolved in 6% HNO_3 and 0.8% HF, and an aliquot of this solution is introduced to the ICPMS via an all-PFA samples introduction system with sapphire injector. Ratios of $^{238}U/^{233}U$ and $^{232}Th/^{229}Th$ are quantified by 2000 measurements of the average intensities in the middle 10% of peakwidths in low resolution mode on an Element2 high-resolution ICP-MS. $^{238}U/^{235}U$ is also measured to check for Pt contamination and mass fractionation. U and Th contents of zircons are calculated from multiple determinations of isotope ratios on pure spike and spiked normals containing 1–4 ng of isotopically normal U and Th. Procedural blanks for U and Th are determined by processing empty Nb foil envelopes, and average 2.9 ± 0.9 pg U and 5.6 ± 1.0 pg Th; this is about four to ten times higher than procedural blanks for apatite.

Figure 6 shows 83 single-crystal analyses of zircons from the Fish Canyon Tuff (FCT) analyzed by methods described above; our mean age is 28.3 Ma, and two standard deviations of the population is 2.6 Ma (9.1%). The most precise U/Pb age of FCT zircon is 28.48 ± 0.06 Ma (2σ) (Schmitz and Bowring 2001). There is some debate as to the crystallization and cooling ages of different phases in the FCT (e.g., Lanphere and Baadsgaard 2001; Schmitz and others 2001; Dazé et al. 2003; Schimtz and others 2003). Some chronometers (with nominally lower closure temperatures) yield ages as young as 27.5 Ma (e.g., Lanphere and Baadsgaard 2001), but Schmitz and Bowring (2001) argue against a prolonged magmatic residence origin for this discrepancy, and several studies suggest systematic ^{40}K decay constant errors may be partly responsible (Min et al. 2000; Kwon et al. 2002). In any case, this uncertainty in FCT ages is well within even one standard deviation of the observed zircon He ages (~1.3 Ma).

Age calculation considerations unique to zircon He dating. Several additional considerations may be necessary in zircon He dating. One that has been recognized for some time is the potential for He age inaccuracies via intracrystalline zonation of U and Th (Farley et al. 1996; Reiners et al. 2004; Hourigan et al. 2005). This problem is not unique to zircon, but because intracrystalline zonation in zircon may be particularly strong, it may be particularly important in some cases of systematic zonation. Strongly heterogeneous distribution of U and Th within crystals affects the alpha-ejection correction because, at least as conventionally applied, this correction assumes uniform distribution of parent nuclides. In the extreme, if all parent nuclides are located on the rim of a crystal, the fraction of alphas retained due to ejection would be slightly less than 0.5 (depending on crystal geometry and size). Conversely
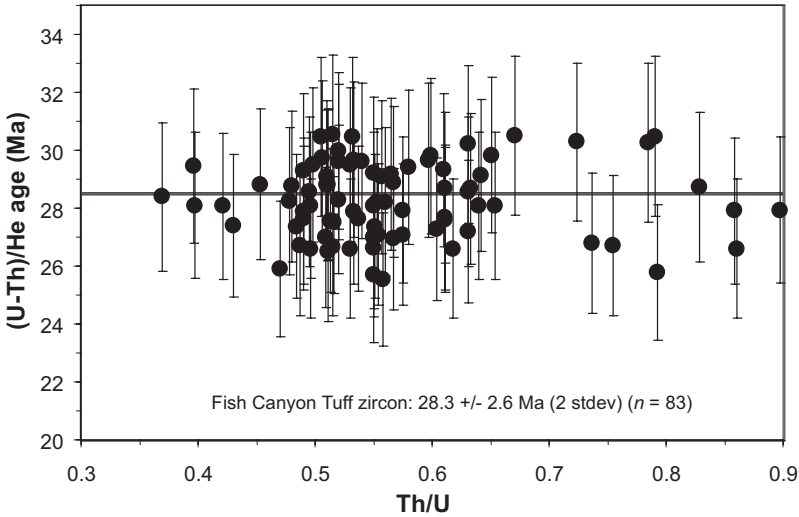
Figure 6. (U-Th)/He ages of 83 single-crystal Fish Canyon Tuff zircons plotted against Th/U, analyzed by procedures described in this chapter, involving Nd:YAG heating of grains in Nb foil, followed by Parr bomb dissolution, and isotope dilution on a high-resolution ICP-MS. The mean age is 28.3 Ma, and two-standard-deviation range of the population is 2.6 Ma (9%). The horizontal grey bar shows the ID-TIMS age and uncertainty of FCT zircon given by Schmitz and Bowring (2001): 28.48 ± 0.06 Ma (2σ).

if all parents are located more than one alpha stopping distance from the rim, no correction would be needed for this effect ($F_{He} = 1$). In practice however, the maximum age inaccuracy that could occur for the most extreme zonation for the vast majority of potential crystal sizes is about 35%, and this decreases with increasing crystal size above about 60 μm prism width.

Hourigan et al. (2005) examined the effects of U-Th zonation on zircon He age inaccuracies for a wide variety of crystal morphologies and styles and extents of zonation. Zircons with U-Th enriched cores produce significantly "too-old" ages (if homogeneous U-Th distributions were assumed in the alpha-ejection correction) with maximum inaccuracies for depleted rims about one stopping distance thick (Fig. 7). The magnitude of this effect however, decreases rapidly as the depleted rim becomes thinner. Enriched rims, however, pose potentially significant age inaccuracies ("too-young" ages) even if they are only 1–2 μm wide. One way to deal with the potential effects of zonation in practice is to examine images of common zonation types and extents in populations of grains exposed in polished mounts and assume similar features in specific grains selected from the population for dating. This approach is often not realistic, however, because of the large variety of zonation exhibited in single samples, especially for detrital samples. Another approach is simply to perform multiple single-crystal age determinations on single samples, though this may not rule out systematic zonation. Hourigan et al. (2005) have developed methods for grain-specific characterization of U-Th zonation by depth profiling in one-dimensional core-to-rim laser ablation pits in crystals selected for dating. These depth-profiles can be converted to zonation models for arbitrary patterns and used to derive customized alpha-ejection corrections specific to each grain. This approach has shown promise for ameliorating systematic age inaccuracies in problematic specimens (Reiners et al. 2004; Hourigan et al. 2005), although complex zonation patterns may still pose problems. Finally, another method under development is characterization of two-dimensional zonation patterns in dated grains by selecting zircons from mounts used for fission-track dating.
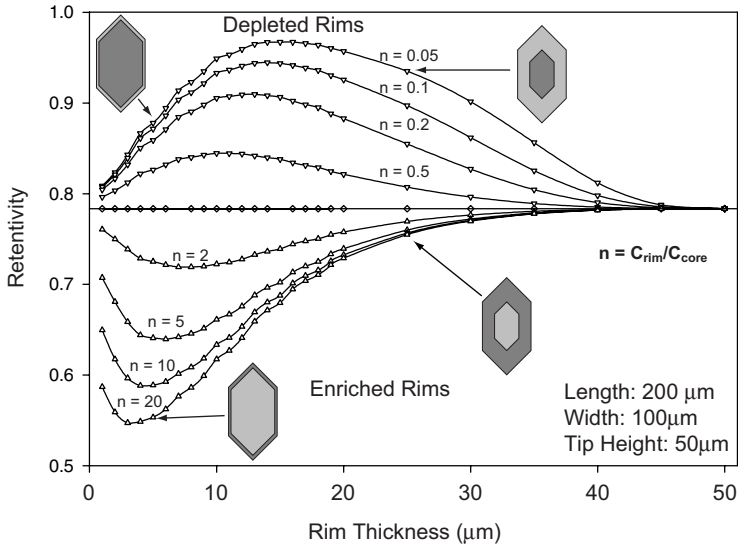
Figure 7. Zoning-dependent bulk retentivity plots for tetragonal model crystals with rims (concentration step functions) of variable width and degree of enrichment or depletion, after Hourigan et al. (2005). The model crystal is a tetragonal prism 200 × 100 μm, with pyramidal terminations (tip height = 50 μm). Although step-function, concentric zonation is obviously a simplification to natural zonation in zircons, this model provides an indication of the magnitudes and styles of zonation required for significant age inaccuracies. Zircons with U-Th enriched rims will show maximum age inaccuracies (as high as about 40% for this morphology) when rims are thin (~2–5 μm), but those with U-Th depleted rims show maximum age inaccuracies (~25%) when rims are about one alpha-stopping-distance thick.

Another consideration that may be important for detrital zircons is the effect of natural abrasion of crystals during transport, and the removal of all or part of the alpha-ejection depleted rim of the crystal. This problem was treated by Rahl et al. (2003) in their study of highly rounded aeolian zircons of the Navajo sandstone. In some cases, abrasion may be so significant that alpha-ejection should only be applied to the post-depositional history of the crystal. Rahl et al.'s equation for a modified post-depositional alpha-ejection corrected age A_c, is:

$$A_c = A_d \left(1 - F_{He}\right) + A_m \tag{4}$$

where A_d is the depositional age of the host sedimentary rock, F_{He} is the standard alpha-ejection correction factor as described above, and A_m is the measured age as determined from relative abundances of parent and daughter nuclides

The relatively high U-Th concentrations of most zircons make zircon He dating potentially useful for dating young (10^3–10^5 ka) volcanic rocks, in age ranges that may be difficult to access by other techniques, as demonstrated by Farley et al. (2002). In such cases, however, consideration of the effects of secular disequilibrium are necessary. Zircon typically has U/Th greater than unity, and thus may exclude ^{230}Th relative to ^{238}U during crystallization. Establishment of secular equilibrium between ^{238}U and ^{230}Th occurs only after about five half-lives of ^{230}Th, or ~375 kyr. For zircons with initial activity ratios of (^{230}Th/^{238}U) < 1, He will be produced at a slower rate for the first ~375 kyr following crystallization, and zircon He ages in this range may be several percent to several tens of percent too-young, depending on the age. As shown by Farley et al. (2002), correction for this secular disequilibrium requires knowledge of (^{230}Th/^{238}U) of the melt from which the zircon crystallized, which may be

constrained by analyzing Th/U of cogenetic phases that fractionate Th/U differently, such as apatite and zircon. An additional important consideration is the magma residence time of crystallized phases, which, for zircon, may be typically about 100–500 kyr (Halliday et al. 1989; Reid et al. 1997; Hawkesworth et al. 2000), comparable with the duration of time required for establishment of secular equilibrium, or longer.

It is worth noting that only when (U-Th)/He ages reflect formation, as opposed to cooling, ages, is consideration of secular equilibrium required. Numerous examples of Holocene through Pleistocene zircon He ages have been documented that reflect resetting by magmatic heating, hydrocarbon burning, or cooling associated with tectonic or erosional exhumation. In such cases, cooling ages are much younger than formation ages, and, assuming no loss of intermediate daughters during cooling or the resetting event, U-series disequilibria considerations are not necessary.

CASE-STUDY EXAMPLES

Comparison with K-feldspar ^{40}Ar/^{39}Ar cooling models

K-feldspar ^{40}Ar/^{39}Ar age spectra from step-heating degassing experiments are widely used to model thermal histories of rocks between temperatures of about 350–150 °C (Lovera et al. 1989, 1991, 1997, 2002; Richter et al. 1991; Harrison et al. 2005). The ability of K-feldspar to provide continuous time-temperature paths, rather than a single point in the thermal history, arises from the inferred multi-domain or multi-path Ar diffusion behavior exhibited by this mineral. The temperature range of many K-feldspar cooling models overlaps with the closure temperatures for the zircon He system inferred from diffusion experiments. Several studies have presented results of zircon He ages from rocks with K-feldspar ^{40}Ar/^{39}Ar cooling models (Kirby et al. 2002; Reiners et al. 2004; Stockli 2005). Although in most cases K-feldspar models suggested relatively rapid cooling rates through the zircon He closure temperatures, the results showed good agreement between the two techniques in nearly all cases (Fig. 8), suggesting that the experimentally determined He diffusion parameters for zircon and its inferred closure temperatures apply in natural settings. In some cases, although mean zircon He ages calculated from single crystal ages still overlapped with K-feldspar cooling models, some single crystals were displaced to older ages. Some proportion of zircons in these samples displayed fairly extreme intracrystalline U-Th zonation (core-to-rim contrasts up to a factor of ~30), which was suggested as a likely cause of some single grain age discrepancies. As discussed subsequently, severe intracrystalline U-Th zonation may lead to scatter in He ages of any mineral, and in the case of zircon, maximum age inaccuracies by the most extreme zonation would not exceed ~35%.

Dike heating

In certain circumstances, wallrocks adjacent to basaltic dikes provide opportunities to compare experimentally determined thermal sensitivities of thermochronometric systems to their natural behavior in a presumably relatively well controlled setting. Characteristic timescales of thermal histories associated with heating from large (~10 m) dikes are typically 10^2–10^4 yr, providing potential calibration tests at an intermediate timescale between the ~10^{-3}–10^{-1} yr of laboratory experiments and ~10^5–10^7 yr natural tectonic processes. Although uncertainties in detailed intrusion history and thermal properties of magma and wallrocks may prevent robust tests or "natural calibrations" based on such results, these settings provide at least first-order consistency tests, and qualitative comparisons of resetting profiles among different thermochronometers with differing thermal sensitivities. Figure 9 shows fission-track and (U-Th)/He ages of zircon and apatite in a horizontal transect of trondhjemitic wallrocks adjacent to a ~9 m wide vertical dike of basaltic andesite in the Wallowa Mountains of
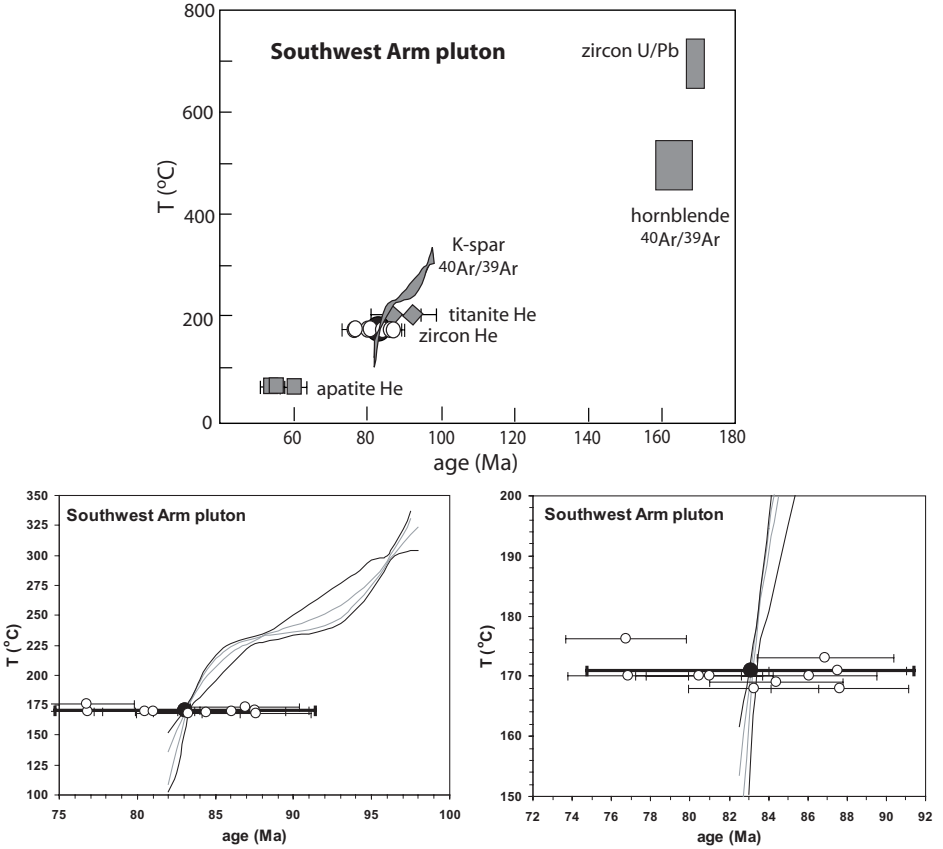
Figure 8. Comparisons between single crystal and averaged zircon He ages and other thermochronometric constraints from the Southwest Arm pluton, Stewart Island, New Zealand (after Reiners et al. 2004). Upper panel: all available data. Lower panels: Detailed comparisons between K-feldspar ^{40}Ar/^{39}Ar cooling models and zircon He ages. White circles are single grain ages; black circles are means. Error bars on single grain ages are 8% (2σ) estimates of reproducibility based on multiple analyses of Fish Canyon Tuff zircon. Error bars on mean ages are two standard deviations of the single grain ages.

northeastern Oregon. Comparisons between high temperature (zircon U/Pb and biotite ^{40}Ar/^{39}Ar) and low-temperature cooling ages in the wallrock at distances greater than ~50 m, as well as other geologic evidence, indicate temperatures less than 40 °C prior to dike intrusion, since the middle Cretaceous. Ages of all four thermochronometers (ZFT, zircon He, AFT, and apatite He) are completely reset to the age of the dike ~17 Ma to a distance of 2 m, and each system shows increasing ages at greater distances, to ~105–120 Ma in unreset portions. To first order, the resetting profiles of each system are similar to those predicted by simple thermal and fractional degassing models based on reasonable thermal properties of the dike and wallrocks. Some discrepancies are observed however, most notably a more complex pattern of resetting in both the ZFT and zircon He systems at distances about 8–15 m from the dike, which requires a more complex thermal evolution at these distance, possibly caused by hydrothermal convection in the wallrock (e.g., Barker et al. 1998), or another heat source out of the plane of exposure. Such a mechanism may also explain why the observed AFT resetting profile is farther from the dike than predicted by simple thermal models. Note, however, that
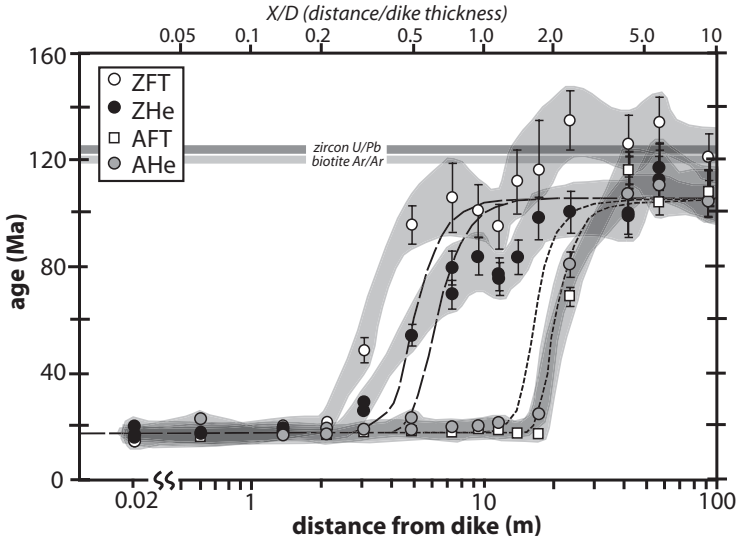
Figure 9. Thermochronometric data for samples adjacent to a ~10 m wide dike of the Columbia River Basalt Group (CRBG), in the Wallowa Mountains of northeastern Oregon. Dashed lines with long and short segments are predicted zircon He and apatite He ages, respectively for dike widths of 8 or 10 m widths (8 m dike predictions are closer to dike margin). Horizontal grey fields show age ranges including 2σ uncertainties on zircon U/Pb (by laser-ablation ICP-MS) ages, and biotite $^{40}Ar/^{39}Ar$ plateau ages. Both ZFT and zircon He ages show decreased ages at about 11–15 m distances from the dike that are not predicted by thermal and diffusion/annealing models. Model assumptions and parameters: Country rock cooling age for zircon He, apatite He, and apatite FT = 105 Ma (based on roughly invariant ages at distances greater than ~40 m from the dike, and other (U-Th)/He ages in the vicinity); dike age = 17 Ma; dike temperature = 1100 °C [typical for CRBG magma; Ho and Cashman (1997)]; country rock temperature between 105 and 17 Ma = 10 °C; thermal diffusivity of country rock and magma = 8.4×10^{-7} m^2/s; heat of fusion of melt in dike = 0.32 MJ/kg; heat capacity of country rock and magma = 1 kJ/kg.

the position of the apatite He profile agrees well with a simple dike heating model, which would not be the case if extra heat were required to explain the ZFT/zircon He patterns or the shifted AFT profile. In summary, dike heating experiments such as this and others (Hart 1964; Wartho et al. 2001) can probably only provide qualitative checks on the thermal sensitivity of thermochronometers, due to uncertainties in a range of parameters, though they are useful as qualitative tests of interchronometer consistency for thermal processes operating at timescales intermediate between laboratory and many tectonic processes.

Exhumed crustal sections

Crustal sections exposed in footwalls of large normal faults provide an opportunity to compare cooling ages of multiple thermochronometers in rocks that have experienced conceivably simple thermal histories that may be simply related by a single geothermal gradient and exhumation history. Typically, these crustal sections are interpreted in the context of long periods of steady-state conditions with little or no cooling/exhumation, producing a partial retention or partial annealing zone (PRZ or PAZ), followed by an episode of rapid tectonic exhumation by hanging wall removal and isostatically-induced tilting/uplift of the footwall.

One example of a tectonically exhumed crustal section is the Gold Butte block in southeastern Nevada, which, on the basis of structural and thermobarometric evidence, has been proposed to be the deepest continuous section of continental crust in the southwestern

U.S. (Fryxell et al. 1992). Apatite fission-track (Fitzgerald et al. 1991), and apatite, titanite, and zircon (U-Th)/He studies (Reiners et al. 2000, 2002) have shown that each thermochronometer records invariant ages at relatively deep paleodepths, and increasingly older ages at shallower paleodepths (Fig. 10). The shallow parts of each trend have been interpreted as partial retention zones developed during a long period of tectonic and erosional quiescence from the Jurassic through Miocene, and the young and invariant ages at depth as recording rapid exhumation during mid-Miocene Basin and Range extension. The break-in-slope in a plot of paleodepth versus zircon He ages is difficult to resolve given zircon abundance in the critical paleodepths, but corresponds to an approximate pre-exhumational temperature of about 180–250 °C, assuming a pre-exhumational geothermal gradient of 20–25 °C/km, consistent with age-paleodepth relations of lower temperature thermochronometers.

At least two potential complications to this simple interpretation of the Gold Butte data exist, however. First, it has been noted (Bernet 2002) that the depth range of the upper section showing a correlation between age and paleodepth is greater than expected for a static PRZ. Bernet (2002) suggested that the upper section instead records slow erosional exhumation of a missing ~4 km section of sedimentary rocks that are no longer preserved in this region. If this is correct, then an apparent break-in-slope would represent the base of a moving, not static PRZ, though it would still correspond approximately to the depth of the closure isotherm at the
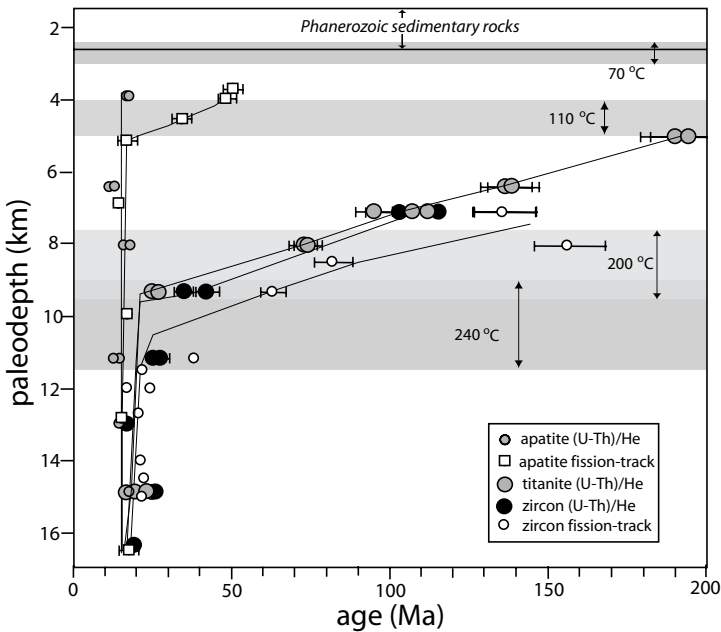

Figure 10. Thermochronologic data from the Gold Butte block, southern Nevada. AFT data are from Fitzgerald et al.(2000), apatite He and titanite He from Reiners et al. (2000), zircon He from Reiners et al. (2002), and ZFT data are from Bernet (2002). Each system except apatite He shows a correlation between age and paleodepth (as determined from distance from and dip of overlying sedimentary rock units) at relatively shallow paleodepths, underlain by young and roughly invariant ages at greater paleodepth. The apatite He system shows roughly constant ages throughout the block. These data have been interpreted to represent slow exhumation-related cooling prior to about 15 Ma, at which time rapid top-down cooling occurred in response to tectonic exhumation of the footwall by normal faulting. Vertical arrows and grey bars show paleodepths of given isotherms, assuming paleogeothermal gradients between 20–25 °C/km.

onset of rapid Miocene extension. The second complication is essentially the possibility that the normal fault that exhumed the Gold Butte footwall changed dip with depth, in which case the apparent paleodepth and temperature at any position in the block may not be easily related by distance from overlying sedimentary units. In this scenario, a listric normal fault would shallow with depth, so paleodepths in the structurally lower part of the block would be less than inferred from their position. Further detailed thermobarometric and higher-temperature thermochronologic work could address this.

Another example of an exhumed crustal section that can be used as either an empirical check on the effective closure depth (and, by inference, closure temperature) of the zircon He system, or else to constrain timing and rate of Miocene exhumation, is the Wassuk range of western Nevada (Tagami et al. 2003; Stockli 2005). This range exposes a paleodepth of approximately 8.5 km, and shows *en echelon* sets of PRZs for the apatite He and zircon He systems, and a PAZ for the AFT system (Fig. 11). The age versus paleodepth data appear to show relatively rapid exhumation-related cooling in the early Paleogene, followed by either slow or no exhumation-related cooling until ~15 Ma, when exhumation rates again increased. Stockli et al. (2002) have estimated pre-15-Ma geothermal gradients of about 26–30 °C/km for this section, which, combined with a paleosurface temperature of ~10 °C and assuming a closure temperature of 180 °C for zircon He, would predict an effective closure depth of the zircon He system of about 5.7–6.5 km. There is a distinct break-in-slope in the Wassuk zircon He data at about 6.5 km (Fig. 11), in good agreement with the prediction based on estimates of the zircon He closure temperature and the pre-exhumation geothermal gradient.
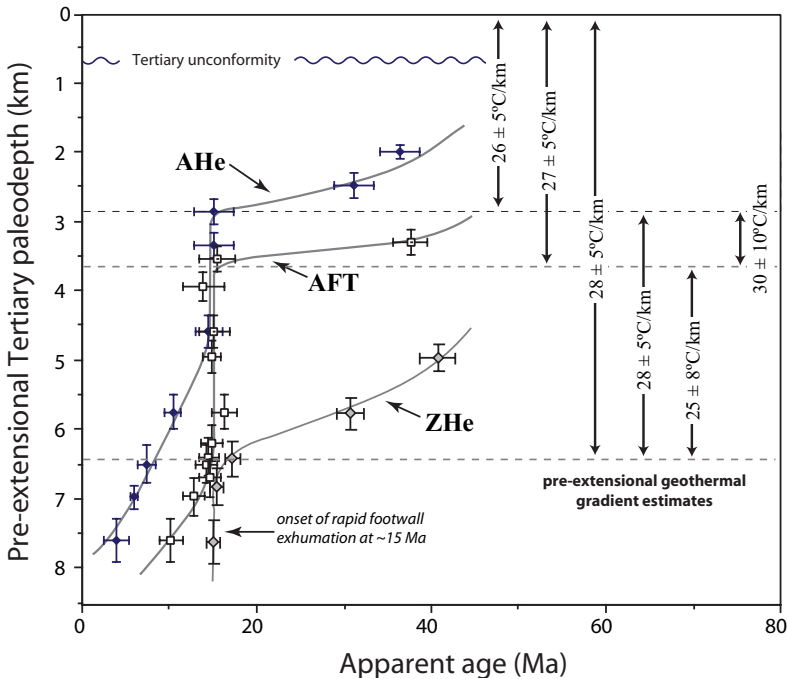

Figure 11. Apatite He, AFT, and zircon He data from the Wassuk crustal section, western Nevada (Stockli 2005). These data show extremely systematic relationships with paleodepth that have been interpreted similarly to those in Figure 10, with slow cooling prior to 15 Ma, at which time the block was rapidly exhumed, quenching thermochronometric ages in all three systems. See Stockli (2005) for further details.

Orogenic exhumation: Dabie Shan

The Dabie Shan was the focus of one of the first regional applications of zircon He thermochronology, combined with other low-temperature thermochronometers (Reiners et al. 2003; see also Kirby et al. 2002). This mountain range is a relatively low-relief (< 1.5 km) orogen in eastern China along part of the early Mesozoic collision zone between the north and south China blocks. The Dabie Shan is famous for its ultra-high pressure (UHP) metamorphic rocks, and its high through intermediate temperature geochronology and thermochronology is well studied by U/Pb and ^{40}Ar/^{39}Ar methods. Following collision and exhumation of UHP rocks in the Triassic-Jurassic (Hacker et al. 2000; Grimmer et al. 2003), Cretaceous granitoids were intruded into a large region of the orogen and this was accompanied by locally high-grade metamorphism at the presently exposed crustal depth (Ratschbacher et al. 2000). Post-orogenic evolution of the range since the Cretaceous has been characterized by slow erosion rates and little tectonism, although Grimmer et al. (2002) invoked early-mid-Tertiary exhumation on the east side of the range based on AFT length modeling.

Figure 12 shows two different ways of representing orogen-scale spatial-temporal patterns of exhumation in the Dabie Shan, using zircon He data combined with AFT and apatite He. Figure 12a shows cooling ages of each system projected onto a horizontal transect across the range, along with a topographic profile. Both zircon and apatite He ages show generally younger ages in the center of the orogen, where mean elevations are the highest. This pattern is consistent with higher long-term erosion rates in the core of the range than on the flanks. A simple model to estimate erosion rates from the zircon He, AFT, and apatite He ages in the core of the range assuming a geothermal gradient of 25 °C/km and closure temperatures of 180 °C, 110 °C and 65 °C, respectively, yields long-term average rates of about 0.07 km/m.y., and slower rates, by about a factor of two, on the range flanks. Figure 12b shows ages of all three systems from samples in a vertical transect in the core of the range. For apatite He ages, the ages are plotted against sample elevation. For AFT and zircon He ages, each sample's elevation is adjusted to a "pseudo-elevation," which is sample elevation plus the ratio between the zircon He-apatite He or AFT-apatite He closure temperature difference and geothermal gradient. This effectively converts each system to a common closure temperature and paleodepth, simulating a single age-elevation trend that would be measured for a single system, if such a high-relief vertical transect existed. This plot shows a steep age-elevation trend at the highest pseudo-elevations (oldest zircon He samples) suggesting rapidly exhumation at about 100 Ma, overlying a trend of roughly constant slope to the lowest pseudo-elevations and youngest ages. A best fit line through the apatite He and AFT data has a slope of about 0.07 km/m.y.. A detailed finite-element model by Braun and Robert (in press) also concluded that an average erosion rate of about 0.07 km/m.y. in the core of the range best explains these data. One potential complication to these data, and a factor that was not considered by Reiners et al. (2003) is the possibility for non-monotonic cooling histories for rocks of the Dabie Shan, involving reburial and reheating following early Mesozoic exhumation.

Detrital zircon dating

Zircon's resilience to weathering and alteration during transport and diagenesis makes it particularly useful in detrital settings, for providing constraints on provenance and depositional age of clastic sedimentary rocks, and for deducing long-term orogenic histories of source terranes. This has been well-established by the long history of U/Pb and fission-track dating studies of detrital zircons (e.g., Wilde et al. 2001; Bernet and Garver 2005). In comparison, few (U-Th)/He dating studies of detrital zircon exist. Those that do have focused on combining multiple radioisotopic techniques on single detrital crystals. For example, Rahl et al. (2003) combined U/Pb dating of ~30 μm deep pits on the crystal exteriors by laser ablation ICP-MS, with subsequent bulk-grain zircon He age determination, to perform
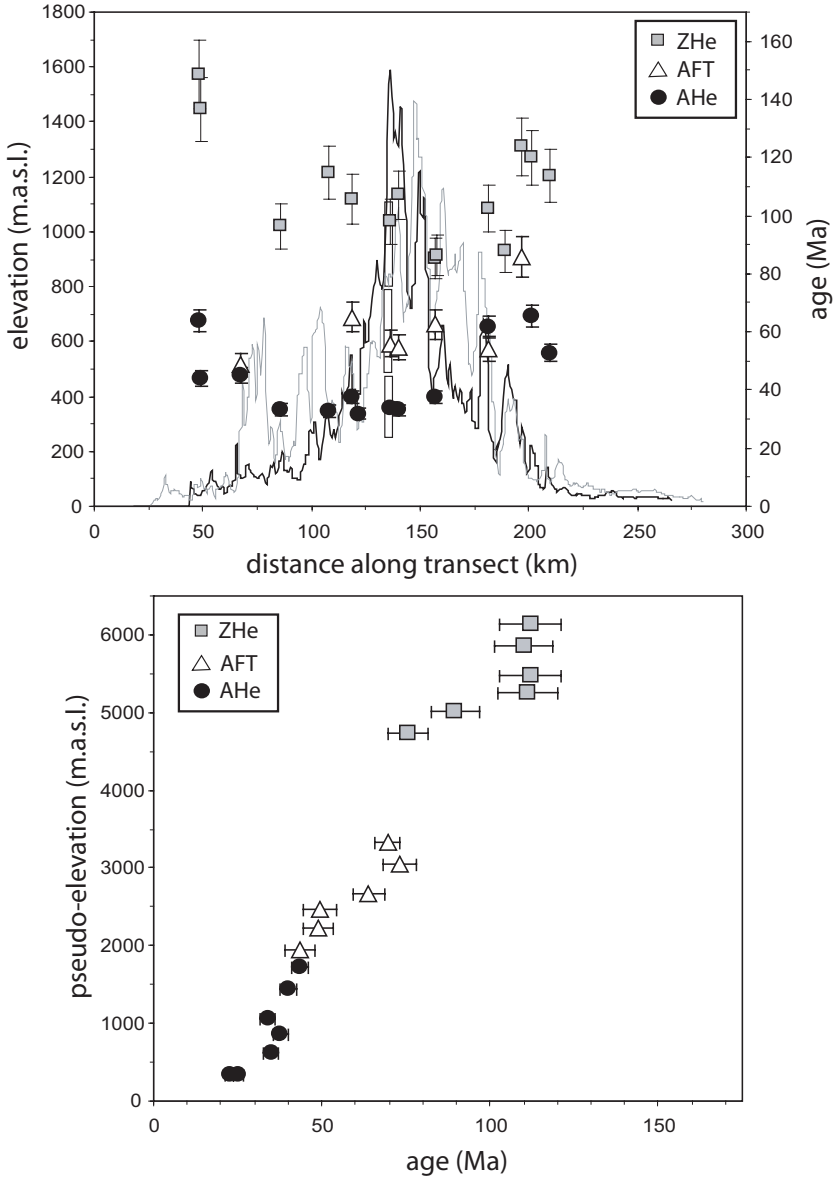
Figure 12. (A) Topography and zircon He, AFT, and apatite He ages projected onto a horizontal transect through the approximate center of the Dabie Shan, from southwest to northeast. Both zircon He and apatite He ages are systematically younger in the core of the range, in the location of the highest topography, consistent with higher long-term erosion rates there, after Reiners et al. (2003). Vertically-stretched boxes in center of range denote age ranges exhibited by samples in a single vertical transect there. (B) Age versus pseudo-elevation plot for zircon He, AFT, and apatite He data from a single vertical transect located in the central part of the Dabie Shan. Pseudo-elevations for the AFT and zircon He systems are shifted in proportion to the difference between their closure temperature and that of the apatite He system. This shows an apparent thermal history involving relatively rapid cooling at ~100 Ma, followed by slow cooling, consistent with an exhumation rate of about 0.07 km/m.y., through the present.

"He-Pb double-dating" of single detrital zircons from the Navajo sandstone in southern Utah. They showed that most of the zircons, and by inference most of the material, in this large erg deposit in the southwestern U.S. was derived from sources with combined U/Pb and He ages most characteristic of the Appalachian-Caledonide orogen of eastern North America (also see Dickinson and Gehrels 2003). In particular, a large population of zircons in these samples had distinctive combinations of ~1.0–1.2 Ga U/Pb ages with ~300–500 Ma He ages. Rahl et al. (2003) suggested that this reflected source rocks formed in the Grenvillian orogeny, but ultimately exhumed and cooled below ~180 °C in the Appalachian-Caledonide orogeny.

Other examples of He-Pb double dating include studies of zircons in active margin flysches in the Olympic Mountains and Kamchatka Peninsula, and Paleogene paleofluvial deposits in northeastern Oregon (Reiners et al. 2005). Campbell et al. (2005) extended He-Pb double-dating to measurement of distinct core and rim U/Pb ages, in addition to bulk grain He ages, on single crystal zircons from the Ganges and Indus rivers. This latter study showed U/Pb ages ranging from ~20–3000 Ma, roughly 70% of which had He ages less than 5 Ma, requiring high exhumation rates of diverse lithologies in the Himalayan source rocks.

Recent developments in detrital zircon dating have expanded to dating of single grains by three separate techniques: U/Pb, ZFT, and zircon He. Figure 13 shows compiled U/Pb, ZFT, and zircon He ages obtained on single grains from the Missouri River, along with He-Pb double-dates on zircons from the Mississippi River and the Navajo Sandstone.
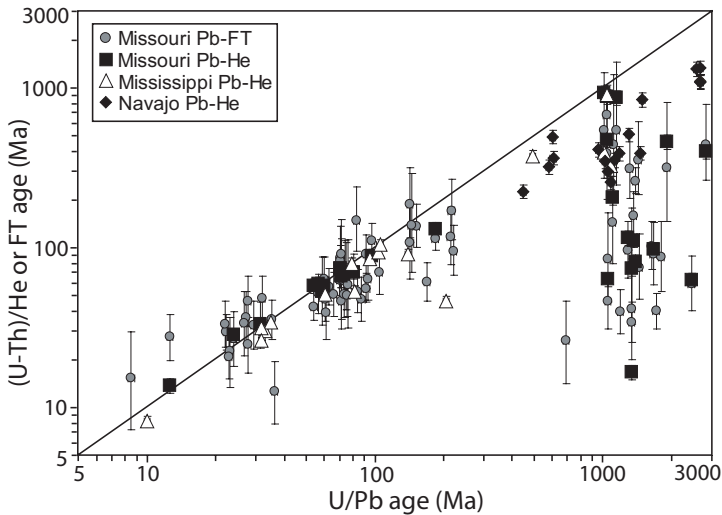

Figure 13. Zircon He and fission-track ages versus U/Pb ages in single zircon crystals from the Missouri and Mississippi rivers, and the Navajo sandstone. Mississippi river and Navajo sandstone zircons are He-Pb double-dates only; Missouri river zircons are He-FT-Pb triple-dates, though not all zircons have been dated by zircon He. Most zircons from both rivers have both crystallization and cooling ages less than 105 Ma, and most of these are close to the first-cycle volcanic trend of identical He and Pb ages. The lack of rocks with such characteristics in the eastern and central parts of North America suggest that most of this detritus in both rivers is derived from the western U.S. Three clusters of young zircons are seen, with potential "magmatic gaps" separating each. A much older group of Precambrian zircons shows a wide range of zircon He ages. Most of the zircons with Grenvillian U/Pb ages show Appalachian zircon He ages, whereas Mesoproterozoic zircons typically have younger cooling ages, corresponding to uplift and exhumation in the Mesozoic-Paleogene Cordilleran orogeny in western North America. Navajo sandstone data are from Rahl et al. (2003).

Most zircons in the modern sediment of these rivers have both U/Pb and He ages less than 105 Ma, and most of these have He ages that are close to or indistinguishable from the U/Pb ages. This is true for the Mississippi, as well as the Missouri, and the near absence of mid-Cretaceous and younger igneous east of the Rockies/Great Plains require that most of the Mississippi's detritus is derived from the western U.S.

Within the dominant population of zircons younger than 105 Ma, there are three clusters of zircons that fall along or near to the first-cycle trend: those with U/Pb ages of about 8–15 Ma, 22–35 Ma, and 55–105 Ma. The lack of zircons with U/Pb ages between 35 and 55 Ma is particularly well pronounced and is likely to represent a "magmatic gap" in the U.S. Cordillera. Of these three younger age groups, the 55–105 Ma group appears to contain the largest number of grains that fall significantly below the first-cycle volcanic trend, with apparent lag times of 20–40 m.y., possibly indicating slow cooling of plutonic rocks or burial and reheating prior to ultimate exhumation for these source rocks.

A fourth group of Phanerozoic zircons is observed in both rivers, with U/Pb ages between about 140 and 220 Ma. Most of these zircons have apparent Pb-He lag times as high as 100–150 m.y. implying slow exhumation or multicycle histories. With the exception of two zircons with U/Pb ages of 0.5 and 0.7 Ga, there is a very pronounced gap in U/Pb ages between ~220 Ma and 1.0 Ga. Precambrian zircons with ages between 1.0–2.8 Ga are abundant in the Missouri and Mississippi rivers. This group shows a hint of an inverse correlation between U/Pb and He ages, caused by the fact that most zircons with 0.9–1.2 Ga U/Pb ages have He ages of ~300–600 Ma, whereas most zircons with U/Pb ages older than ~1.2 Ga have He ages younger than 150 Ma. The zircons with Grenvillian U/Pb ages and Appalachian He ages are almost certainly derived from eastern North America. The presence of these grains in Missouri river sediment is probably due to transport and multi-cycle burial of grains derived from eastern North America, in the western part of the continent, as in the case of the Navajo sandstone. Zircons with Mesoproterozoic U/Pb ages but He ages less than ~150 Ma probably represent sources in the Belt Supergroup and related units, and possibly Ancestral Rockies uplifts, that were ultimately exhumed and cooled in Mesozoic through Paleogene Cordilleran orogenic events.

FUTURE DEVELOPMENTS

Zircon's relatively high abundance in diverse lithologies, high U concentrations, and fairly well-understood thermal sensitivity, make it a promising geo- and thermochronometric target for innovative He dating approaches in a wide range of applications. One example is using zircon He ages to constrain the timing, duration, intensity, and spatial patterns of natural surface or subsurface fires. Zircon He ages have been used to identify the effects of wildfire heating in exposed bedrock (Mitchell and Reiners 2003), and to map the spatial-temporal patterns of natural coalfire that have occurred in the Great Plains since the Pliocene (Heffern and Coates 2004), creating metamorphosed rocks known as clinker. Clinker has been dated by zircon He methods as young as ~10 ka in the Powder River basin of Wyoming and Montana, and the spatial patterns of clinker ages show systematic relationships with respect to topography that hold promise for constraining landscape evolution over timescales of 10^3–10^6 yr. Another promising aspect of using zircon He dating to identify surface reheating signals arises from the relative kinematics of He diffusion and fission-track annealing in zircon. As is also the case in apatite, at relatively short timescales and high temperatures, fission-tracks anneal more rapidly than He diffuses (Fig. 14). This leads to FT ages that are younger than He ages, a diagnostic indicator of short-duration reheating events that holds promise for elucidating volcanic processes (Stockli et al. 2000), shear heating along faults (e.g., Tagami 2005), and the distributions and dynamics of paleowildfire (Reiners and Donelick 2004).
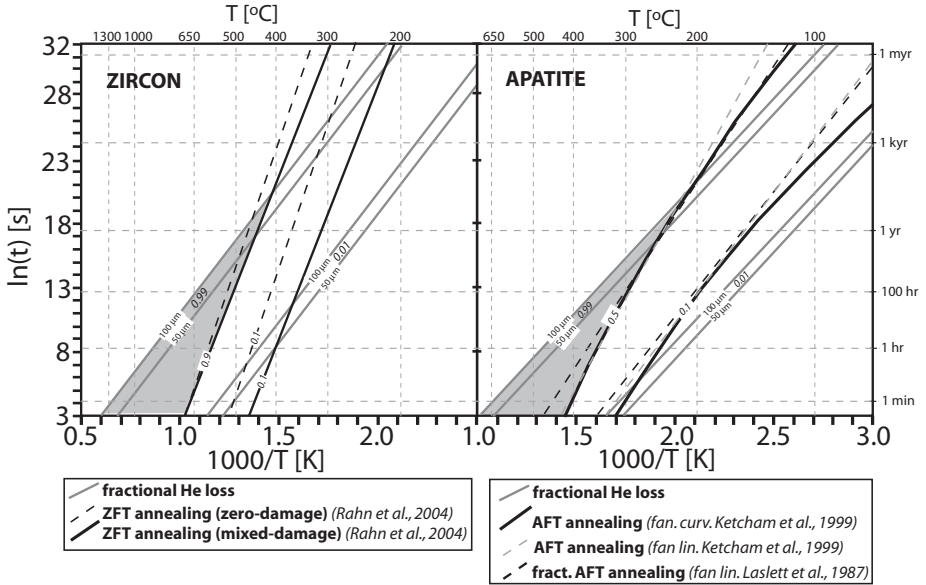
Figure 14. Pseudo-Arrhenius plots for He diffusion and fission-track shortening, relating time, temperature, and fractional degassing or track shortening for stepwise heating events. Solid grey lines denote fractional He degassing of 1.0% and 99% for spherical diffusion domain radii of 50 and 100 μm. AFT and ZFT contours are fractional fission-track shortening of 0.1 and 0.5 (at which point track density rapidly decreases), and 0.1 and 0.9, respectively. He diffusion parameters are from Farley (2000) for apatite, and Reiners et al. (2004) for zircon. Differing activation energies of the He and FT systems lead to "inverted" He-FT age relationships (He age older than FT age, or partially reset He age with fully reset FT age, the latter shown by shaded area) after short duration heating events. This is a diagnostic indicator of wildfire or other short-timescale, near-surface thermal events.

Another particularly promising prospect for zircon He dating is the potential to obtain spatially-resolved He concentrations or ages within single crystals. Just as ion probe and laser-ablation ICP-MS techniques allow discrimination of distinct U/Pb ages in rim and core portions of detrital zircons, advances in He dating techniques may soon allow in situ determinations of intracrystalline He age or concentration variations. Although no technique can currently measure both He and U-Th contents in precisely the same micro-analytical pit, two methods pose considerable promise. One is ^{4}He/^{3}He thermochronometry (e.g., Shuster and Farley 2005), whereby homogeneous ^{3}He distributions are generated throughout crystals by proton bombardment, and the evolution of ^{4}He/^{3}He in gas fractions released during step heating experiments is used to model detailed thermal histories of crystals. This technique has been successfully applied to several minerals, and assuming intracrystalline U-Th zonation issues could be addressed, it should be suitable for zircon as well. Another technique that may be able to directly measure in situ age distributions comes from the use of high-precision and -accuracy excimer laser ablation and He analysis of small (~5–10 μm) pits in core-to-rim traverses across single grains, followed by U-Th analyses in the same, or parallel, traverses, as suggested by Hodges and Boyce (2003). Again assuming that complications arising from the combined effects of U-Th zonation and the ~17 μm alpha-stopping distances can be addressed, this approach should allow estimation of not only bulk crystal closure ages, but also intracrystalline closure profiles (Dodson 1986), providing continuous time-temperature paths and constraints on cooling rates of the source rocks, as is done in K-feldspar ^{40}Ar/^{39}Ar and

monazite U/Pb thermochronometry (e.g., Harrison et al. 2005). Zircon may prove particularly useful for this type of approach, because of the potentially high He contents needed to overcome blanks in small laser-ablation pits within crystals.

ACKNOWLEDGMENTS

REFERENCES

Barker CE, Bone Y, Lewan MD (1998) Fluid inclusion and vitrinite-reflectance geothermometry compared to heat-flow models of maximum paleotemperature next to dikes, western onshore Gippsland Basin, Australia. Int J Coal Geol 37:73-111

Bernet M (2002) Exhuming the Alps through time: Clues from detrital zircon fission-track ages. PhD Dissertation, Yale University, New Haven, Connecticut

Bernet M, Garver JI (2005) Fission-track analysis of detrital zircon. Rev Mineral Geochem 58:205-238

Brandon MT, Vance JA (1992) Tectonic evolution of the Cenozoic Olympic subduction complex, Washington State, as deduced from fission track ages for detrital zircons. Am J Sci 292:565-636

Bowring SA, Schmitz MD (2003) High-precision U-Pb zircon geochronology and the stratigraphic record. Rev Mineral Geochem 53:305-326

Braun J, Robert X (in press) Constraints on the rate of post-orogenic erosional decay from low temperature thermochronological data: application to the Dabie Shan, China. Earth Surf Proc Land.

Campbell IH, Reiners PW, Allen C, Nicolescu S, Upahdyay R (2005) He-Pb double-dating of detrital zircons from the Ganges and Indus rivers: Implication for quantifying sediment recycling, exhumation rates and provenance studies, Earth Planet Sci Lett, in press

Dazé A, Lee JKW, Villeneuve M (2003) An intercalibration study of the Fish Canyon sanidine and biotite [40]Ar/[39]Ar standards and some comments on the age of the Fish Canyon Tuff. Chem Geol 199:111-127

Dickinson WR, Gehrels GE (2003) U–Pb ages of detrital zircons from Permian and Jurassic aeolian sandstones of the Colorado Plateau, USA: paleogeographic implications. Sed Geol 163:29-66

Dodson MH (1973) Closure temperature in cooling geochronological and petrological systems. Contrib Mineral Petrol 40:259-274

Dodson MH (1979) Theory of cooling ages. *In:* Lectures in Isotope Geology. Jäger E, Hunziker JC (eds) Springer-Verlag, Berlin, p 194-202

Dodson MH (1986) Closure profiles in cooling systems. *In:* Materials Science Forum. Vol. 7. Trans Tech Publications, Aedermannsdorf, Switzerland. p 145-153

Ehlers TA, Farley KA (2003) Apatite (U-Th)/He thermochronometry: methods and applications to problems in tectonics and surface processes. Earth Planet Sci Lett 206:1-14

Farley KA (2000) Helium diffusion from apatite: General behavior as illustrated by Durango fluorapatite. J Geophys Res 105:2903-2914

Farley KA (2002) (U-Th)/He dating: techniques, calibrations, and applications. Rev Mineral Geochem 47: 819-844

Farley KA, Stockli DF (2002) (U-Th)/He dating of phosphates: apatite, monazite, and xenotime. Rev Mineral Geochem 48:559-577

Farley KA, Wolf RA, Silver LT (1996) The effects of long alpha-stopping distances on (U-Th)/He ages. Geochim Cosmochim Acta 60:4223-4229

Farley KA, Kohn BP, Pillans B (2002) The effects of secular disequilibrium on (U–Th)/He systematics and dating of Quaternary volcanic zircon and apatite. Earth Planet Sci Lett 201:117-125

Fitzgerald PG, Fryxell JE, Wernicke BP (1991) Miocene crustal extension and uplift in southeastern Nevada: Constraints from fission track analysis. Geology 10:1013-1016

Fryxell JE, Salton GG, Selverstone J, Wernicke B (1992) Gold Butte crustal section, South Virgin Mountains, Nevada. Tectonics 11:1099-1120

Futa K (1986) Sm-Nd systematics of a tonalitic augen gneiss and its constituent minerals from northern Michigan. Geochim Cosmochim Acta 45:1245-1249

Gerling EK (1939) Diffusion temperature of helium as a criterion for the usefulness of minerals for helium age determination. Compt Red Acad Sci URSS 24:570-573

Grimmer JC, Jonckheere R, Enkelmann E, Ratschbacher L, Hacker BR, Blythe AE, Wagner GA, Wu Q, Liu S, Dong S (2002) Cretaceous-Cenozoic history of the southern Tan-Lu fault zone: apatite fission-track and structural constraints from the Dabie Shan (eastern China). Tectonophy 359:225–253

Grimmer JC, Ratschbacher L, McWilliams M, Franz L, Gaitzch I, Tichomirowa M, Hacker BR, Zhang Y (2003) When did the ultra-high pressure rocks reach the surface? A ^{207}Pb/^{206}Pb zircon, ^{40}Ar/^{39}Ar white mica, Si-in-white mica, single-grain provenance study of Dabie Shan synorogenic foreland sediments. Chem Geol 197:87–110

Hacker BR, Ratschbacher L, Webb L, McWilliams MO, Ireland T, Calvert A, Dong S, Wenk HR, Chateigner D (2000) Exhumation of ultrahigh-pressure continental crust in east central China: Late Triassic-Early Jurassic tectonic unroofing. J Geophys Res 105:13,339–13,364

Halliday AN, Mahood GA, Holden P, Metz JM, Dempster TJ, Davidson JP(1989) Evidence for long residence times of rhyolitic magma in the Long Valley magmatic system—the isotopic record in precaldera lavas of Glass Mountain. Earth Planet Sci Lett 94:274–290

Harrison TM, Grove M, Lovera OM, Zeitler PK (2005) Continuous thermal histories from inversion of closure profiles. Rev Mineral Geochem 58:389-409

Hawkesworth CJ, Blake S, Evans P, Hughes R, MacDonald R, Thomas LE, Turner SP, Zellmer G (2000) Time scales of crystal fractionation in magma chambers—integrating physical, isotopic and geochemical perspectives. J Petrol 41:991–1006

Hart SR (1964) The petrology and isotopic-mineral age relations of a contact zone in the Front Range, Colorado. J Geol 72:493-525

Heffern EL, Coates DA (2004) Geologic history of natural coalbed fires, Powder River Basin, USA. Int J Coal Geol 59:25-47

Ho AM, Cashman KV (1997) Temperature constraints on the Gingko flow of the Columbia River Basalt Group. Geology 25:403-406

Hodges K, Boyce J (2003) Eos, Trans, Am Geophys U 84(46), Fall Meeting Supplement, Abstract V22G-05

Holland HD (1954) Radiation damage and its use in age determination. *In*: Nuclear Geology. Faul H (ed) Wiley, New York, p 175–179

Holland HD, Gottfried D (1955) The effect of nuclear radiation on the structure of zircon. Acta Crystallogr 8: 291–300

Holmes A, Paneth FA (1936) Helium-ratios of rocks and minerals from the diamond pipes of South Africa. Proc Roy Soc Lond A154:385-413

Hourigan JK, Reiners PW, Brandon MT (2005) U-Th zonation dependent alpha-ejection in (U-Th)/He chronometry, Part I: Theory. Geochim Cosmochim Acta 69:3349-3365

House MA, Farley KA, Stockli D (2000) Helium chronometry of apatite and titanite using Nd-YAG laser heating. Earth Planet Sci Lett 183:365-368

Hurley PM (1952) Alpha ionization damage as a cause of low helium ratios. Trans Am Geophys U 33:174-183

Hurley PM (1954) The helium age method and the distribution and migration of helium in rocks. *In*: Nuclear Geology. Faul H (ed) Wiley, New York, p 301-329

Hurley PM, Fairbairn HW (1953) Radiation damage in zircons: a possible age method. Bull Geol Soc Am 64: 659-674

Hurley PM, Larsen ES Jr., Gottfried D (1956) Comparison of radiogenic helium and lead in zircon. Geochim Cosmochim Acta 9:98-102

Ireland TR, Williams IS (2003) Considerations in zircon geochronology by SIMS. Rev Mineral Geochem 53: 215-241

Keevil NB, Larsen ES Jr., Wank FJ (1944) Distribution of helium and radioactivity in rocks. VI: The Ayer granite-migmatite at Chelmsford, Mass. Am J Sci 242:345-353

Ketcham RA, Donelick RA, Carlson WD (1999) Variability of apatite fission-track annealing kinetics: III. Extrapolation to geological time scales. Am Mineral 84:1235-1255

Kirby E, Reiners PW, Krol M, Hodges K, Farley KA, Whipple K, Yiping L, Tang W, Chen Z (2002) Late Cenozoic uplift and landscape evolution along the eastern margin of the Tibetan plateau: Inferences from ^{40}Ar/^{39}Ar and U-Th-He thermochronology. Tectonics 10.1029/2000TC001246

Larsen ES Jr., Keevil NB (1942) The distribution of helium and radioactivity in rocks. III: Radioactivity and petrology of some California intrusives. Am J Sci 240:204-215

Larsen ES, Keevil NB, Harrison HC (1952) Method for determining the age of igneous rocks using the accessory minerals. Geol Soc Am Bull 63:1045-1052

Laslett GM, Green PF, Duddy IR, Gleadow AJW (1987) Thermal annealing of fission tracks in apatite. 2. A quantitative analysis. Chem Geol (Isot Geosci Sect) 65:1-13

Lovera OM, Richter FM, Harrison TM (1989) The ^{40}Ar/^{39}Ar thermochronometry for slowly cooled samples having a distribution of diffusion domain sizes. J Geophys Res 94:17917-17935

Lovera OM, Richter FM, Harrison TM (1991) Diffusion domains determined by ^{39}Ar released during step heating. J Geophys Res 96:2057-2069

Lovera OM, Grove M, Harrison TM (2002) Systematic analysis of K-feldspar ^{40}Ar/^{39}Ar step heating results II: Relevance of laboratory argon diffusion properties to nature. Geochim Cosmochim Acta 66:1237-1255

Lovera OM, Grove M, Harrison TM, Mahon KI (1997) Systematic analysis of K-feldspar ^{40}Ar/^{39}Ar step heating results. 1. Significance of activation energy determinations. Geochim Cosmochim Acta 61: 3171-3192

Mitchell SG, Reiners PW (2003) Influence of wildfires on apatite and zircon (U-Th)/He ages. Geology 31: 1025-1028

Naeser CW, Zimmermann RA, Cebula GT (1981) Fission-track dating of apatite and zircon: An interlaboratory comparison. Nucl Tracks 5:65-72

Nasdala L, Reiners PW, Garver JI, Kennedy AK, Stern RA, Balan E, Wirth R (2004) Incomplete retention of radiation damage in zircon from Sri Lanka. Am Mineral 89:219-231

Nasdala L, Wenzel M, Vavra G, Irmer G, Wenzel T, Kober B (2001) Metamictisation of natural zircon: accumulation versus thermal annealing of radioactivity-induced damage. Contrib Mineral Petrol 141: 125–144

Parrish RR, Noble SR (2003) Zircon U-Th-Pb geochronology by isotope dilution—thermal ionization mass spectrometry (ID-TIMS). Rev Mineral Geochem 53:183-213

Pettingill HS, Patchett PJ (1981) Lu-Hf total-rock age for the Amîtsoq gneisses, West Greenland. Earth Planet Sci Lett 55:150-156

Pik R, Marty B, Carignan J, Lave J (2003) Stability of the Upper Nile drainage network (Ethiopia) deduced from (U-Th)/He thermochronometry: implications for uplift and erosion of the Afar plume dome. Earth Planet Sci Lett 215:73-88

Rahl JM, Reiners PW, Campbell IH, Nicolescu S, Allen CM (2003) Combined single-grain (U-Th)/He and U/Pb dating of detrital zircons from the Navajo Sandstone, Utah. Geology 31:761-764

Rahn, MK, Brandon MT, Batt GE, Garver JI (2004) A zero-damage model for fission-track annealing in zircon Am Mineral 89:473-484

Ratschbacher L, Hacker BR, Webb LE, McWilliams M, Ireland T, Dong S, Calvert A, Chateigner D, Wenk HR (2000) Exhumation of the ultrahigh-pressure continental crust in east central China: Cretaceous and Cenozoic unroofing and the Tan-Lu fault. J Geophys Res 105:13,303–13,338

Reid MR, Coath CD, Harrison TM, McKeegan KD (1997) Prolonged residence times for the youngest rhyolites associated with Long Valley Caldera: ^{230}Th-^{238}U ion microprobe dating of young zircons. Earth Planet Sci Lett 150:27–39

Reiners PW, Brady R, Farley KA, Fryxell JE, Wernicke BP, Lux D (2000) Helium and argon thermochronometry of the Gold Butte block, South Virgin Mountains, Nevada. Earth Planet Sci Lett 178:315-326

Reiners PW, Campbell IH, Nicolescu S, Allen CA, Hourigan JK, Garver JI, Mattinson JM, Cowan DS (2005) (U-Th)/(He-Pb) "double-dating" of detrital zircons. Am J Sci 305:259-311

Reiners PW, Donelick RA (2004) Thermochronology of wildfire and fault heating through single grain (U-Th)/He and fission-track double dating. Geol Soc Am Abstr Prog Vol. 36, No. 5, p. 447

Reiners PW, Farley KA (1999) He diffusion and (U-Th)/He thermochronometry of titanite. Geochim Cosmochim Acta 63:3845-3859

Reiners PW, Farley KA (2001) Influence of crystal size on apatite (U-Th)/He thermochronology: an example from the Bighorn Mountains, Wyoming. Earth Planet Sci Lett 188:413-420

Reiners PW, Farley KA, Hickes HJ (2002) He diffusion and (U-Th)/He thermochronometry of zircon: Initial results from Fish Canyon Tuff and Gold Butte. Tectonophys 349:247-308

Reiners PW, Spell TL, Nicolescu S, Zanetti KA (2004) Zircon (U-Th)/He thermochronometry: He diffusion and comparisons with ^{40}Ar/^{39}Ar dating. Geochim Cosmochim Acta 68:1857-1887

Reiners PW, Zhou Z, Ehlers TA, Xu C, Brandon MT, Donelick RA, Nicolescu S (2003) Post-orogenic evolution of the Dabie Shan, eastern China, from (U-Th)/He and fission-track dating. Am J Sci 303:489-518

Richter FM, Lovera OM, Harrison TM, Copeland P (1991) Tibetan tectonics from [40]Ar/[39]Ar analysis of a single K-feldspar sample. Earth Planet Sci Lett 105:266-278

Schärer U (1984) The effect of initial [230]Th disequilibrium on young U-Pb ages: the Makalu case, Himalaya. Earth Planet Sci Lett 67:191–204

Schmitz MD, Bowring SA (2001) U-Pb zircon and titanite systematics of the Fish Canyon Tuff: an assessment of high precision U-Pb geochronology and its application to young volcanic rocks. Geochim Cosmochim Acta 65:2571-2587

Seitz F (1949) On the disordering of solids by action of fast massive particles. Disc Far Soc 5:271-282

Shuster DL, Farley KA (2004) [4]He/[3]He thermochronometry. Earth Planet Sci Lett 217:1-17

Shuster DL, Farley KA, Sisterson JM, Burnett DS (2004) Quantifying the diffusion kinetics and spatial distributions of radiogenic [4]He in minerals containing proton-induced [3]He. Earth Planet Sci Lett 217: 19-32

Silver LT, Deutsch S (1963) Uranium-lead isotopic variations in zircons: a case study. J Geol 71:721-758

Stockli DF (2005) Application of low-temperature thermochronometry to extensional tectonic settings. Rev Mineral Geochem 58:411-448

Stockli DF, Farley KA (2004) Empirical constraints on the titanite (U–Th)/He partial retention zone from the KTB drill hole. Chem Geol 227:223-236

Stockli DF, Farley KA, Dumitru TA (2000) Calibration of the apatite (U-Th)/He thermochronometer on an exhumed fault block, White Mountains, California. Geology 28:983-986

Stockli DF, Surpless BE, Dumitru TA, Farley KA (2002) Thermochronological constraints on the timing and magnitude of Miocene and Pliocene extension in the central Wassuk Range, western Nevada. Tectonics 21:4, doi: 10.1029/2001TC001295.02

Strutt RJ (1910a) The accumulation of helium in geologic time, II. Proc Roy Soc Lond, Ser A 83:96-99

Strutt RJ (1910b) The accumulation of helium in geologic time, III. Proc Roy Soc Lond, Ser A 83:298-301

Strutt RJ (1910c) Measurements of the rate at which helium is produced in thorianite and pitchblende, with a minimum estimate of their antiquity. Proc Roy Soc Lond, Ser A 83:379-388

Tagami T, Farley KA, Stockli DF (2003) (U-Th)/He geochronology of single zircon grains of known Tertiary eruption age. Earth Planet Sci Lett 207:57-67

Tilton GR, Patterson C, Brown H, Inghram M, Hayden R, Hess D, Larsen E (1955) Isotopic composition and distribution of lead, uranium and thorium in a Precambrian granite. Geol Soc Am Bull 66:1131-1148

Turner G, Harrison TM, Holland G, Mojzsis SJ, Gilmour J (2004) Extinct [244]Pu in ancient zircons. Science 306:89-91

Vinogradov AP, Zadorozhnyi IK, Zykor SI (1952) Isotopic composition of lead and the age of the earth. Dokl Akad Nauk SSSR 85:1107-1110

Wartho J-A, Kelley SP, Blake S (2001) Magma flow regimes in sills deduced from Ar isotope systematics of host rocks J Geophys Res 106:4017-4035

Webber GR, Hurley PM, Fairbairn HW (1956) Relative ages of eastern Massachusetts granites by total lead ratios in zircon. Am J Sci 254:574-583

Wernicke B, Getty SR (1997) Intracrustal subduction and gravity currents in the deep crust: Sm-Nd, Ar-Ar, and thermobarometric constraints from the Skagit Gneiss Complex, Washington. Geol Soc Am Bull 109: 1149-1166

Wetherill GW (1955) An interpretation of the Rhodesia and Witwatersrand age patterns. Geochim Cosmochim Acta 9:290-292

Wilde SA, Valley JW, Peck WH, Graham CM (2001) Evidence from detrital zircons for the existence of continental crust and oceans on the Earth 4.4 Gyr ago. Nature 409:175-178

Wolf RA, Farley KA, Silver LT (1996) Helium diffusion and low-temperature thermochronometry of apatite. Geochim Cosmochim Acta 60:4231-4240

Wolf RA, Farley KA, Kass DM (1998) Modeling of the temperature sensitivity of the apatite (U-Th)/He thermochronometer. Chem Geol 148:105-114

Zeitler PK, Herczeg AL, McDougall I, Honda M (1987) U-Th-He dating of apatite: a potential thermochronometer. Geochim Cosmochim Acta 51:2865-2868